NAVAL POSTGRADUATE SCHOOL

MONTEREY, CALIFORNIA

THESIS

DEMODULATION OF OFDM SIGNALS IN THE PRESENCE OF DEEP FADING CHANNELS AND SIGNAL CLIPPING

by

Konstantinos Charisis

June 2012

Thesis Advisor:	Roberto Cristi
Thesis Co-Advisors:	Monique P. Fargues
	Tri Ha

Approved for public release; distribution is unlimited

THIS PAGE INTENTIONALLY LEFT BLANK

REPORT DOCUMENTATION PAGE			Form Approved OMB No. 0704-0188
Public reporting burden for this collection of information is estimated to average 1 hour per response, including the time for reviewing instruction, searching existing data sources, gathering and maintaining the data needed, and completing and reviewing the collection of information. Send comments regarding this burden estimate or any other aspect of this collection of information, including suggestions for reducing this burden, to Washington headquarters Services, Directorate for Information Operations and Reports, 1215 Jefferson Davis Highway, Suite 1204, Arlington, VA 22202-4302, and to the Office of Management and Budget, Paperwork Reduction Project (0704-0188) Washington DC 20503.			
1. AGENCY USE ONLY *(Leave blank)*	**2. REPORT DATE** June 2012	**3. REPORT TYPE AND DATES COVERED** Engineer's and Master's Thesis	
4. TITLE AND SUBTITLE Demodulation of OFDM Signals in the Presence of Deep Fading Channels and Signal Clipping		**5. FUNDING NUMBERS**	
6. AUTHOR(S) Konstantinos Charisis			
7. PERFORMING ORGANIZATION NAME(S) AND ADDRESS(ES) Naval Postgraduate School Monterey, CA 93943-5000		**8. PERFORMING ORGANIZATION REPORT NUMBER**	
9. SPONSORING /MONITORING AGENCY NAME(S) AND ADDRESS(ES) N/A		**10. SPONSORING/MONITORING AGENCY REPORT NUMBER**	
11. SUPPLEMENTARY NOTES The views expressed in this thesis are those of the author and do not reflect the official policy or position of the Department of Defense or the U.S. Government. IRB Protocol number _____N/A_____.			
12a. DISTRIBUTION / AVAILABILITY STATEMENT Approved for public release; distribution is unlimited		**12b. DISTRIBUTION CODE**	

13. ABSTRACT (maximum 200 words)

In this thesis, an optimal estimation algorithm, based on the Kalman Filter, is introduced for data recovery of orthogonal frequency-division multiplexed (OFDM) signals transmitted over fading channels. We show that the use of a zero prefix (ZP) along with a fast Fourier transform (FFT) operation zero padded to twice the data length allows for the recovery of subcarriers located next to a deep faded (at low signal-to-noise ratio [SNR]) values, exploiting all other subcarriers with higher SNR. The same approach is also shown to improve demodulation in the presence of signal clipping due to high peak to average power ratio (PAPR), as is often seen in OFDM signals.

The proposed method assumes prior knowledge of the channel, usually estimated using the preamble. Testing was conducted for random channels with zero frequency response at a random frequency ω_0 and a signal in additive white Gaussian noise for various conditions. Further testing was done with typical Stanford University Interim (SUI) channels.

Additionally, the use of the method to recover OFDM signals based on the IEEE 802.11 and 802.16 standards was examined. Results show that the proposed optimal estimation algorithm has very satisfactory performance compared to the standard OFDM receiver algorithm.

14. SUBJECT TERMS Wireless Communications, Fading Channels, Kalman Filter, OFDM, PAPR, Zero-Prefix.			**15. NUMBER OF PAGES** 77
			16. PRICE CODE
17. SECURITY CLASSIFICATION OF REPORT Unclassified	**18. SECURITY CLASSIFICATION OF THIS PAGE** Unclassified	**19. SECURITY CLASSIFICATION OF ABSTRACT** Unclassified	**20. LIMITATION OF ABSTRACT** UU

NSN 7540-01-280-5500 Standard Form 298 (Rev. 2-89)
Prescribed by ANSI Std. 239-18

THIS PAGE INTENTIONALLY LEFT BLANK

Approved for public release; distribution is unlimited

DEMODULATION OF OFDM SIGNALS IN THE PRESENCE OF DEEP FADING CHANNELS AND SIGNAL CLIPPING

Konstantinos Charisis
Lieutenant, Hellenic Navy
B.S., Hellenic Naval Academy, 2002

Submitted in partial fulfillment of the
requirements for the degree of

ELECTRICAL ENGINEER
and
MASTER OF SCIENCE IN ELECTRICAL ENGINEERING

from the

NAVAL POSTGRADUATE SCHOOL
June 2012

Author: Konstantinos Charisis

Approved by: Roberto Cristi
Thesis Advisor

Monique P. Fargues
Thesis Co-Advisor

Tri Ha
Thesis Co-Advisor

R. Clark Robertson
Chair, Department of Electrical and Computer Engineering

THIS PAGE INTENTIONALLY LEFT BLANK

ABSTRACT

In this thesis, an optimal estimation algorithm, based on the Kalman Filter, is introduced for data recovery of orthogonal frequency-division multiplexed (OFDM) signals transmitted over fading channels. We show that the use of a zero prefix (ZP) along with a fast Fourier transform (FFT) operation zero padded to twice the data length allows for the recovery of subcarriers located next to a deep faded (at low signal-to-noise ratio [SNR]) values, exploiting all other subcarriers with higher SNR. The same approach is also shown to improve demodulation in the presence of signal clipping due to high peak to average power ratio (PAPR), as is often seen in OFDM signals.

The proposed method assumes prior knowledge of the channel, usually estimated using the preamble. Testing was conducted for random channels with zero frequency response at a random frequency ω_0 and a signal in additive white Gaussian noise for various conditions. Further testing was done with typical Stanford University Interim (SUI) channels.

Additionally, the use of the method to recover OFDM signals based on the IEEE 802.11 and 802.16 standards was examined. Results show that the proposed optimal estimation algorithm has very satisfactory performance compared to the standard OFDM receiver algorithm.

THIS PAGE INTENTIONALLY LEFT BLANK

TABLE OF CONTENTS

THIS PAGE INTENTIONALLY LEFT BLANK

LIST OF FIGURES

LIST OF TABLES

THIS PAGE INTENTIONALLY LEFT BLANK

LIST OF ACRONYMS AND ABBREVIATIONS

AWGN	Additive White Gaussian Noise
BER	Bit Error Rate
BPSK	Binary Phase-Shift Keying
BWA	Broadband Wireless Access
CP	Cyclic Prefix
DFT	Discrete Fourier Transform
FFT	Fast Fourier Transform
IDFT	Inverse Discrete Fourier Transform
IFFT	Inverse Fast Fourier Transform
ISI	Inter-Symbol Interference
LAN	Local Area Networks
LOS	Line of Sight
LTI	Linear Time Invariant
MAC	Medium Access Control
MIMO	Multiple-Input Multiple-Output
NOLOS	Non Line-of-Sight
OFDM	Orthogonal Frequency-Division Multiplexing
PAPR	Peak-to-Average Power Ratio
QAM	Quadrature Amplitude Modulation
QPSK	Quadrature Phase-Shift-Keying
RF	Radio Frequency
RMS	Root Mean Square
SER	Symbol Error Rate
SIMO	Single-Input Multiple-Output
SISO	Single-Input Single-Output
SNR	Signal-to-Noise Ratio
SUI	Stanford University Interim
WAN	Wide Area Network
WiMAX	Worldwide Interoperability for Microwave Access
ZP	Zero Prefix

THIS PAGE INTENTIONALLY LEFT BLANK

EXECUTIVE SUMMARY

Orthogonal frequency-division multiplexing (OFDM) modulation has become the method of choice for numerous standards such as IEEE 802.11 and IEEE 802.16 in worldwide digital television and many other applications. The reasons for its popularity are its high data rate transmission and ease of demodulation in the presence of multipath fading without the high complexity equalization required in single carrier modulation schemes.

In spite of its effectiveness and wide range of use, OFDM has two major drawbacks. One is due to the fact that the received components from different paths may add constructively at certain frequencies and destructively at others. This causes fading for certain subcarriers, even in the presence of strong received signals, resulting in loss of data at these subcarriers. The second drawback is due to the random nature of OFDM transmitted signals which may present wide amplitude variations resulting in a potentially high peak-to-average power ratio (PAPR). As a result, OFDM based transmitters are designed to limit PAPR to avoid saturation in the amplifier stage.

In this research, we propose a method based on earlier work which uses an OFDM symbol with zero prefix (ZP) instead of the standard cyclic prefix (CP), to recover the data from faded subcarriers. This method uses a longer fast Fourier transform (FFT) at the receiver than that applied in OFDM standard demodulation to exploit the correlation between even and odd frequency components.

The proposed optimal estimation method is based on standard Kalman filtering and combines a priori information of the transmitted symbols with observations made by the FFT of the received data and demodulated non-faded subcarriers. In order to distinguish between faded and non-faded subcarriers, we introduce the notion of an optimal threshold in the frequency domain. Using this threshold, we can discriminate between faded (with low signal-to-noise ratio (SNR) and non-faded (with high SNR) subcarriers. From this point, the demodulated, non-faded subcarriers along with the received signal comprise the observation information used in the optimal estimation algorithm in order to recover the data from the faded subcarriers.

This research goes one step further and shows that the same idea can improve the signal demodulation in the presence of high PAPR. In this thesis we use the solution of clipping by limiting the peak amplitude at the transmitter to some desired maximum level. The chosen clipping method is based on the standard deviation of the transmitted signal. From this reference point, the desired PAPR is the one that defines the maximum allowed peak of the transmitted signal.

The efficiency of the proposed optimal estimation algorithm is tested in this thesis for OFDM signals based on IEEE standards 802.11 and 802.16 for a number of channels. Specifically we used channels under extreme conditions, meaning channels with absolute nulls at one or more frequencies. However, more realistic channels have less severe constraints as their frequency responses might attenuate some frequencies but, in general, every subcarrier carries information. Thus, we also used the third Stanford University Interim (SUI-3) channel model which has some line-of-sight (LOS) characteristics and low spread as well as a modified version with non-line-of-sight (NOLOS) attributes. Simulations were conducted using MATLAB.

The proposed algorithm was also tested under various PAPR conditions to investigate its performances and efficiency for different clipping levels.

Simulations involve three major testing steps. The first step identifies the optimal threshold, defined as that which gives the best results and the best symbol error rate (SER). The second step simulates the algorithm for various channel conditions using the optimal threshold. Finally, we use the optimal estimation algorithm for various PAPR clipping values.

The algorithm performances are compared at every step to those obtained with the standard OFDM receiver algorithm. Results show that the algorithm based on the proposed method overall performs better. In some cases, the proposed optimal estimation algorithm performs better even when the OFDM signal is extremely clipped, in order to deal with the problem of PAPR, as compared to the standard OFDM receiver algorithm, which uses the unclipped signal.

ACKNOWLEDGMENTS

I would like to express my deepest appreciation to my thesis advisor Professor Roberto Cristi and my committee members Professor Monique P. Fargues and Professor Tri Ha for their guidance and suggestions in the completion of this thesis.

I would like to thank my parents, Stelios and Eleni, and my brother, Dimitri, for their endless support and understanding.

THIS PAGE INTENTIONALLY LEFT BLANK

I. INTRODUCTION

A. OVERVIEW

Orthogonal frequency-division multiplexing (OFDM) is a broadband modulation method that allows transmission of high data rates over a wireless channel. OFDM has advantages over traditional single-carrier modulation methods and has become the method of choice for wireless technologies. Its main advantage is that it mitigates the effect of multipath fading, which cause data errors in standard single carrier modulation schemes. OFDM copes with this multipath problem by transmitting data in blocks of narrowband subcarriers and suitable time guards.

Recall that one of the effects of multipath is frequency-selective fading, in which each subcarrier has a different signal-to-noise ratio (SNR). As a consequence, the data in the subcarriers corresponding to "nulls" in the channel frequency response might be lost due to destructive interference between multipath receptions.

B. OBJECTIVES AND METHODOLOGY

It has been shown in [1] that by replacing the cyclic prefix (CP) with zeros, the received signal has a particular structure that can be used to recover the data from faded subcarriers. This is along the lines of recent work in [2], which addresses some improvements in OFDM receivers. The scope of this thesis research is to improve this method using optimal estimation techniques and test the effectiveness in a number of channel conditions.

The main idea behind the proposed algorithm is the fact that in OFDM with zero-prefix (ZP) the whole OFDM symbol (data plus prefix) is processed at the receiver, unlike the standard OFDM with CP, which completely discards the received overhead. In the proposed OFDM ZP case, the received data is processed by a double-length fast Fourier transform (FFT), so that the correlation between even and odd frequency components can be exploited to effectively recover data in the faded subcarriers.

The estimation method implemented in this thesis is based on standard Kalman filtering. It combines a priori information of the transmitted symbols (in general a quadrature phase-shift keyed (QPSK) or a quadrature amplitude modulation (M-QAM) signal) with observations made by the FFT of received data and also by the demodulated, non-faded, high SNR subcarriers. This research examines how accurately the received signal can be recovered for various channel conditions. Simulations are conducted using MATLAB.

A very important issue we address is the choice of an optimal threshold in the frequency domain so that we can discriminate between faded (with low SNR) and non-faded (with high SNR) subcarriers. A QPSK signal is sent through a deep-fading noisy channel, and the aim is to find the optimal threshold so as to optimize the accuracy of the results and minimize the errors.

When this phase is completed, the algorithm is implemented using SIMULINK for real-time implementation and to verify that the results obtained are consistent with those obtained in MATLAB.

An additional feature of the proposed algorithm is the fact that it can improve performance in the presence of the high peak-to-average power ratio (PAPR) inherent in OFDM signals by using clipping. Since clipping introduces wide band noise, faded subcarriers with already low SNR values are more affected than non-faded subcarriers at higher SNR values. The algorithm is tested for different channel conditions and different levels of clipping to show the effectiveness of the proposed approach.

The same set of simulations are conducted for OFDM signals based on the IEEE standards 802.11 and 802.16 for various channel models, including the Stanford University Interim (SUI) channels.

C. ORGANIZATION

The thesis is organized into six chapters. A background discussion on OFDM modulation and its use in current standards is provided in Chapter II. A method of recovering the information lost in deep fading channels is discussed in Chapter III.

Simulations and results of the implementation of this method are presented in Chapters IV and V. Finally, in Chapter VI, a summary of the work conducted in this thesis, results, conclusions and suggestions for future studies are discussed.

THIS PAGE INTENTIONALLY LEFT BLANK

II. OVERVIEW OF OFDM: CYCLIC PREFIX AND ZERO PREFIX

The idea of the OFDM transmission technique is to split the total available bandwidth B into many narrowband sub-channels at equidistant frequencies. The sub-channel spectra overlap each other, but the subcarrier signals are still orthogonal. The single high-rate data stream is subdivided into many low-rate data streams for the sub-channels. Each sub-channel is modulated individually and transmitted simultaneously in a superimposed and parallel form.

In standard OFDM, the transmitted signal is additionally extended by a cyclic prefix (so-called guard interval) of length exceeding the maximum multipath delay in order to avoid inter symbol interference (ISI), as may occur in multipath channels in the transition interval between two adjacent OFDM symbols.

In this thesis we use an OFDM symbol with ZP instead of using CP. This method, with the use of a longer FFT at the receiver, can reliably recover subcarriers with low SNR due to deep fading noisy channels using FFT properties.

In spite of its effectiveness and wide range, OFDM modulation has two major problems. One is due to the fact that received components from different paths may add constructively at certain frequencies and destructively at other frequencies. This behavior causes fading for certain subcarriers even in the presence of strong received signals, with resulting low SNR at these subcarriers.

The other drawback is the random nature of OFDM transmitted signals. Unlike single-carrier QPSK signals where the carrier has a constant magnitude, OFDM signals are more like pseudo-noise and present wide amplitude variations. This is quantified by the PAPR which is large for OFDM signals and forces a reduction in the transmitted power to avoid saturation in the amplifier at the transmitter.

These two issues are at the center of the proposed approach.

A. OFDM SYMBOL

In OFDM each transmitted signal can be defined as

$$s(t) = \mathrm{Re}\left\{ e^{j2\pi F_C t} x(t) \right\} \tag{1}$$

where F_C is the carrier frequency. The complex baseband signal is subdivided into time intervals of length T_{Symbol}. Within the m-th time interval the signal $x(t)$ is defined as

$$x\left(mT_{Symbol} + t\right) = x_m(t) = \sum_{\substack{k=-\frac{N_F}{2} \\ k\neq 0}}^{k=\frac{N_F}{2}} c_k e^{j2\pi k\Delta F t} \quad 0<t \le T_{Symbol} \tag{2}$$

where N_F is the number of subcarriers, c_k depends on the transmitted data and ΔF is defined below. The parameter T_{Symbol} is the symbol length and consists of the guard interval T_g and data interval T_b:

$$T_{Symbol} = T_g + T_b. \tag{3}$$

In order to guarantee the subcarriers to be mutually orthogonal, we choose the difference between the subcarrier frequencies to be integer multiples of

$$\Delta F = \frac{1}{T_b}. \tag{4}$$

In this way, orthogonality of the subcarriers can be easily verified as

$$\frac{1}{T_b}\int_{t_0}^{t_0+T_b} e^{j2\pi F_k t} e^{-j2\pi F_l t} dt = \frac{1}{T_b}\int_{t_0}^{t_0+T_b} e^{j2\pi (k-l)\Delta F t} dt = \begin{cases} 1 & \text{if } k = l \\ 0 & \text{if } k \neq l \end{cases}. \tag{5}$$

For a linear time-invariant (LTI) channel, at least within the symbol duration, and for a guard interval T_g greater than the time spread, the subcarriers are still orthogonal at the receiver and defined by

$$y(t) = \sum_k c_k H\left(F_k\right) e^{j2\pi F_k t} \quad T_g \le t \le T_g + T_b, \tag{6}$$

where $H(F)$ is the frequency response of the channel.

This leads to a very simple discrete time implementation by letting F_s be the sampling frequency, N be the number of data samples in each symbol and $\Delta F = 1/(NT_S) = F_S/N$ be the subcarriers spacing. Then (2) becomes

$$x(nT_S) = \frac{1}{N}\sum_{k=-\frac{N_F}{2}}^{\frac{N_F}{2}} c_k e^{j2\pi k\frac{\Delta F}{F_S}(n-L)} = \frac{1}{N}\sum_{k=-\frac{N_F}{2}}^{\frac{N_F}{2}} c_k e^{jk\frac{2\pi}{N}(n-L)} \quad n = 0,\ldots,L+N-1, \tag{7}$$

where $T_g = LT_S$ is the length in time of the guard interval.

To complete the pre-coding necessary for OFDM, we use the inverse fast Fourier transform. After dropping the block index m for ease of notation, we get

$$\begin{aligned} x[n+L] &= \frac{1}{N}\sum_{k=-\frac{N_F}{2}}^{\frac{N_F}{2}} c_k e^{jk\frac{2\pi}{N}n} = \frac{1}{N}\sum_{k=1}^{\frac{N_F}{2}} c_k e^{jk\frac{2\pi}{N}n} + \frac{1}{N}\sum_{k=-\frac{N_F}{2}}^{-1} c_k e^{j(N+k)\frac{2\pi}{N}n} \\ &= \frac{1}{N}\sum_{k=0}^{N-1} X[k] e^{jk\frac{2\pi}{N}n} = IFFT\{X[k]\} \end{aligned}, \tag{8}$$

where $X[k] = c_k$ is for positive subcarriers $(k>0)$, $X[N+k] = c_k$ is for negative subcarriers $(k<0)$ and $X[k] = 0$ for $k = 0$.

From (2) and the subcarrier frequencies being multiples of ΔF in (4), we see that the data transmitted during the guard interval is a periodic repetition, where the CP are the last L points of the $IFFT\{X[k]\}$.

The demodulation of the OFDM signal is obtained by the convolution of the channel impulse response and the signal as

$$y[n+L] = h[n] * x[n] = h[n] * \frac{1}{N}\sum_{k=0}^{N-1} X[k] e^{j\frac{2\pi}{N}kN}$$
$$= \frac{1}{N}\sum_{k=0}^{N-1} H[k] X[k] e^{j\frac{2\pi}{N}kn} = IFFT\{H[k] X[k]\} \quad , \tag{9}$$

which leads to the result

$$H[k] X[k] = FFT\{y[L], \ldots, y[L+N-1]\}$$
$$\text{with } H[k] = FFT\{h[0], \ldots, h[L-1], 0, \ldots, 0\} \quad k = 0, \ldots, N-1 \; . \tag{10}$$

The block diagram of an OFDM communication system is illustrated in Figure 1.

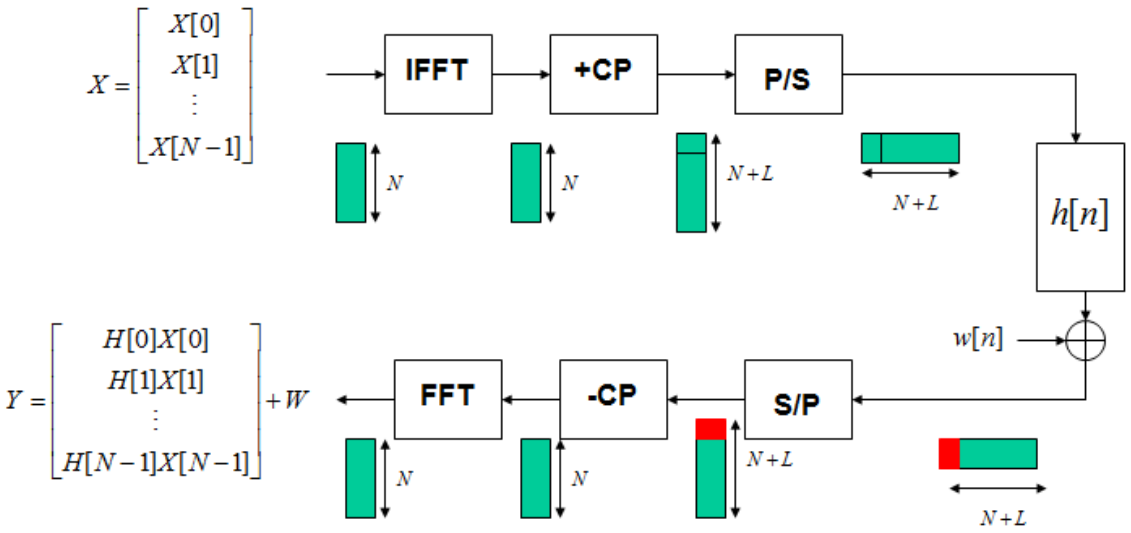

Figure 1. Block diagram of an OFDM communication system. From [3].

The received signal is of the form

$$Y[k] = H[k]X[k] + W[k] \tag{11}$$

where $W[k]$ is the FFT of the additive noise $w[n]$. If the channel frequency response is known, the transmitted signal $X[k]$ can be recovered using a standard Wiener filter as

$$\hat{X}[k] = \frac{H^*[k]}{\left|H[k]^2 + \sigma_W{}^2\right|} Y[k]. \tag{12}$$

The limitation to this approach is that the information in the CP is completely discarded at the receiver and just treated as overhead [3].

The method described in this thesis requires a ZP OFDM symbol and is described further in Chapter III. The main idea is that each transmitted data symbol $x[0],...,x[M-1]$ is followed by a block of L zeros (the ZP) rather than repeating the signal values $x[0],...,x[L-1]$.

Although all standards available today are based on the CP, it has been shown in [1] that simple processing of an OFDM-CP signal results in an OFDM-ZP signal.

The transformation from a CP OFDM signal $y_{CP}[n]$ into a ZP OFDM signal is obtained by subtracting a delayed version of the signal from itself as

$$y_{ZP}[n] = y_{CP}[n] - y_{CP}[n-M]. \tag{13}$$

In Figure 2, it can be seen how CP terms cancel out since the data in the CP is the same as the data at the end of the OFDM symbol.

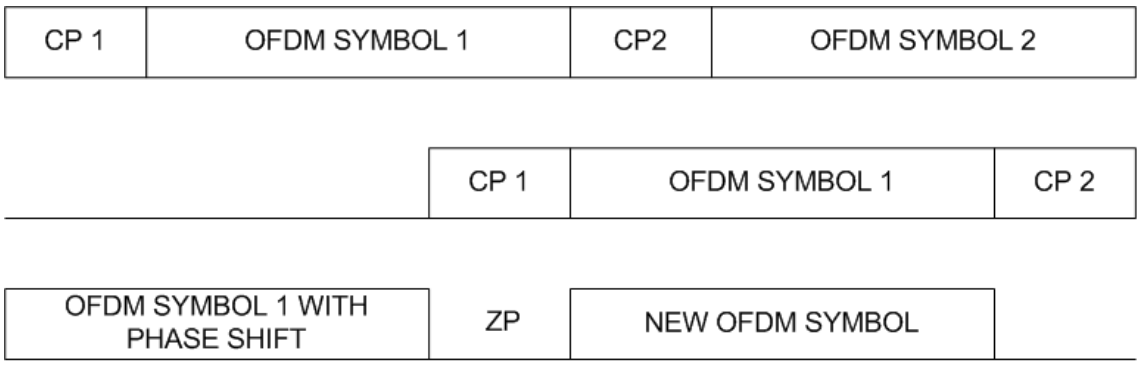

Figure 2. A delay of M points results in a phase shift of the first OFDM symbol with a ZP and new symbols subsequent to that. From [1].

Note that data blocks may be mapped to the individual subcarriers according to a number of standards, each suitable to a different application. In this research we refer to two widely used standards: IEEE 802.11 for local area networks (LAN) and WiFi and IEEE 802.16 for wide area networks (WAN) and WiMax. The two standards are briefly described in the next section.

B. OFDM STANDARDS

1. IEEE Standards 802.11 and 802.16

The IEEE 802.11a standard describes an OFDM physical layer that uses 52 subcarriers to transmit data. Four of the subcarriers are pilot subcarriers, and the remaining 48 carry the data to be transmitted. The frequency spacing ΔF is 0.3125 MHz, where the guard interval is 0.8 μs and the data interval 3.2 μs. In Figure 3, we can see the mapping of the IFFT inputs to the time-domain.

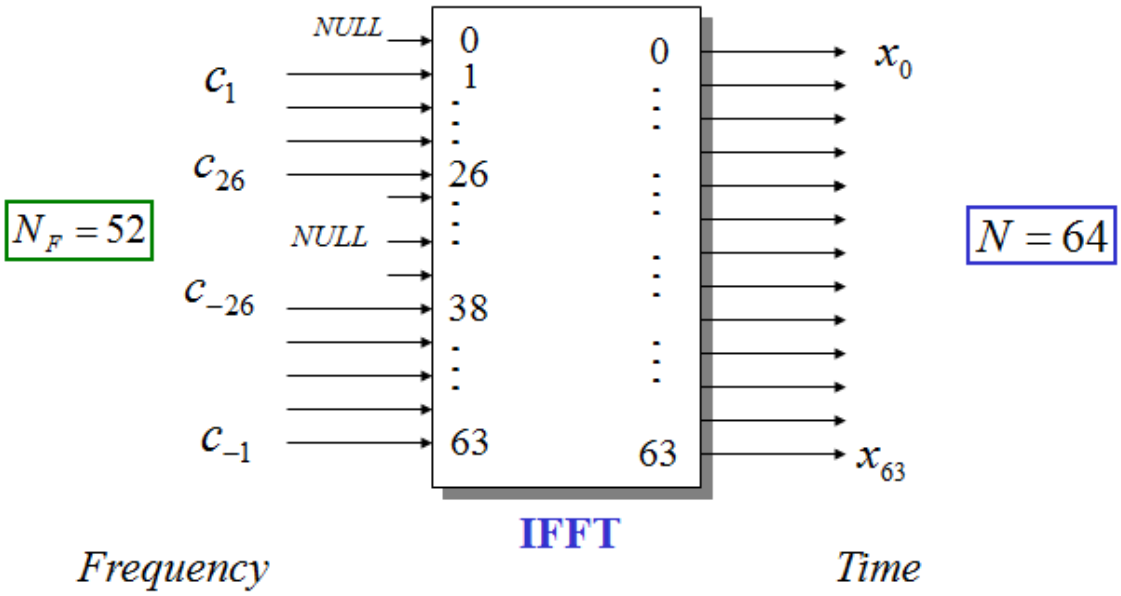

Figure 3. Mapping of the IFFT inputs to time-domain outputs for 802.11a. From [3].

A number of variations and modulations have been introduced. These amendments improve the initial standard.

The IEEE 802.11g standard is an amendment to the IEEE 802.11 specification using the 2.4 GHz band to include OFDM. The input structure is the same as for IEEE 802.11a but with a lower carrier frequency. 802.11g is more promising due to the larger operating distance.

The IEEE 802.11n standard improves the previous standards using multiple-input-multiple-output (MIMO) antennas to achieve higher throughput and operates at both 2.4 GHz and 5 GHz. It can achieve a maximum data rate of 600 Mbps.

The IEEE 802.16 standard specifies the air interface for broadband wireless access (BWA) systems. The IEEE 802.16 medium access control (MAC) protocol is designed for point-to-multipoint BWA systems and for very high bit rates for both uplink and downlink [4].

In Table 1 the parameters set by IEEE 802.16 standards for the OFDM signals is listed.

Table 1. Parameters for IEEE 802.16 (OFDM only). From [3].

	802.16-2004	802.16e-2005
Frequency Band	2GHz-11GHz	2GHz-11GHz fixed 2GHz-6GHz mobile
OFDM carriers	OFDM: 256 OFDMA: 2048	OFDM: 256 OFDMA: 128, 256, 512,1024, 2048
Modulation	QPSK, 16QAM, 64QAM	QPSK, 16QAM, 64QAM
Transmission Rate	1Mbps-75Mbps	1Mbps-75Mbps
Duplexing	TDD or FDD	TDD or FDD
Channel Bandwidth	(1,2,4,8)x1.75MHz (1,4,8,12)x1.25MHz 8.75MHz	(1,2,4,8)x1.75MHz (1,4,8,12)x1.25MHz 8.75MHz

In Figure 4, the subcarrier allocation is illustrated for the case of N = 256 subcarriers. All other settings (N = 512, 1024 or 2048) follow a similar structure.

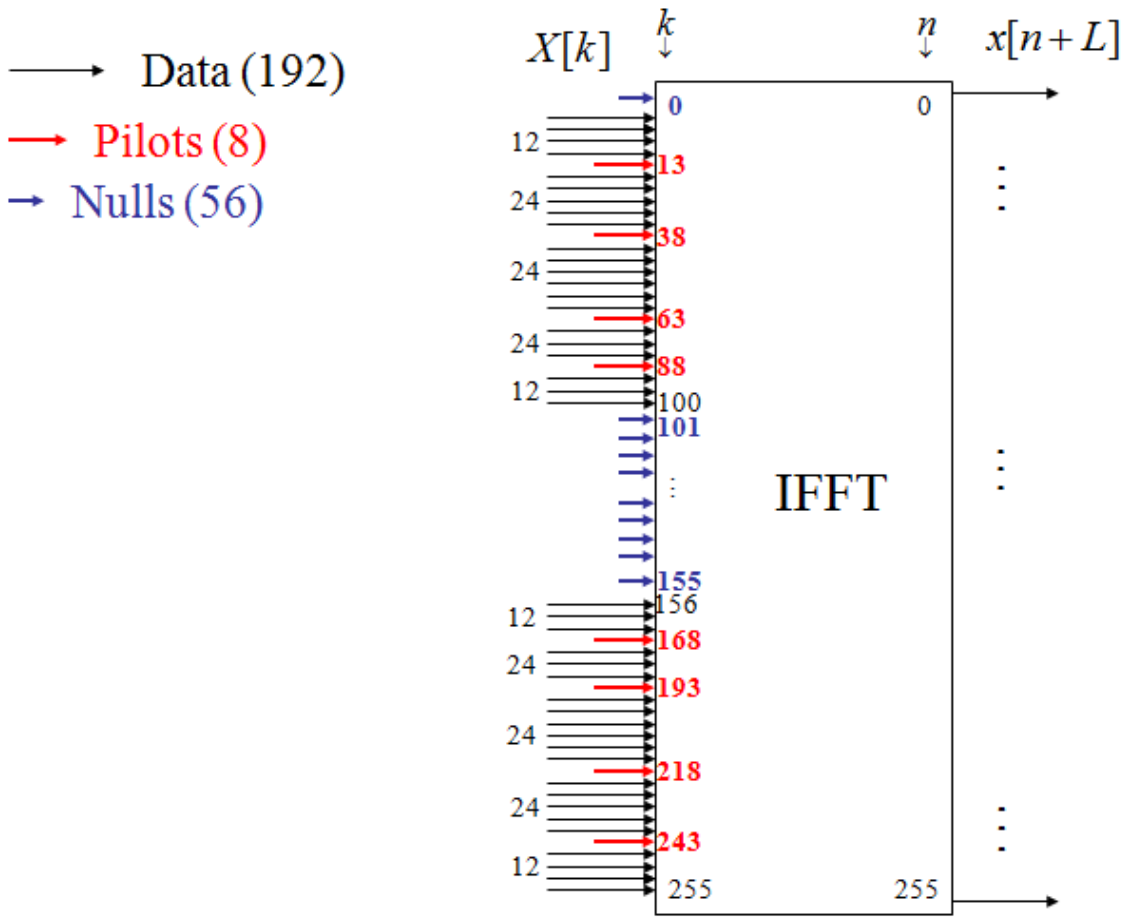

Figure 4. Mapping of the IFFT inputs to time-domain outputs for 802.16 for N=256 subcarriers. From [3].

THIS PAGE INTENTIONALLY LEFT BLANK

III. OPTIMAL ESTIMATION FOR DATA RECOVERY IN THE PRESENCE OF DEEP FADING CHANNELS

In the previous chapter, we have seen that typical wireless channels can be subject to deep fading which, in turn, affects data transmission in a portion of the spectrum. This is particularly important in OFDM where a block of data is transmitted through a number of subcarriers, each occupying a small part of the spectrum. A fading channel in this case causes errors in the data transmitted in the "deep faded" subcarriers.

It was proposed in [1] that by using an OFDM modulator with ZP and a longer FFT size at the demodulator, even and odd subcarriers of the received OFDM symbol can offer sufficient redundancy so that the lost data can be recovered.

The algorithm presented in [1] is a simple deterministic implementation which does not take noise characteristics into account and leads to results which are fairly sensitive to noise at the receiver.

In this chapter, we briefly review the method proposed in [1] and introduce an optimal estimation method (based on the Kalman Filter) which can be used to achieve better results.

A. DATA RECOVERY FROM A FADED SUBCARRIER USING NULL ESTIMATION

In OFDM with ZP, each transmitted symbol can be written as

$$x = \left[x[0], x[1], ..., x[M-1], 0, ..., 0 \right] \tag{14}$$

where x is a vector of length P which includes the data symbols $x[0],\ldots,x[M-1]$ and the ZP of L zeros at the end. Although "prefix" indicates "before the symbol", in this case we use a "suffix" after the symbol for convenience. The distinction is actually immaterial since in both cases we simply alternate data and zeros.

The M point DFT and the $2M$ point (zero padded) discrete Fourier transform (DFT) of the transmitted data are defined as

$$X_M[k] = DFT\{[x[0],...,x[M-1]]\}, \quad k = 0,...,M-1$$
$$X_{2M}[m] = DFT\{[x[0],...,x[M-1]],0,0,...,0\}, \quad m = 0,...,2M-1 \qquad (15)$$

where M zeros are added to x before the $2M$ point DFT is taken.

The block diagram of a ZP OFDM communication system is illustrated in Figure 5.

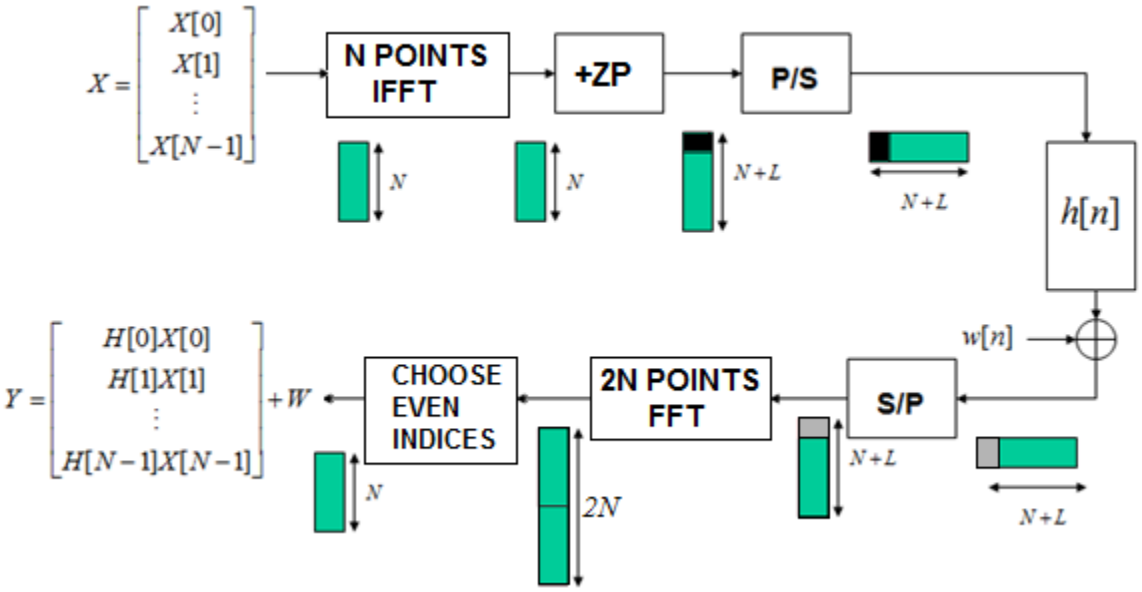

Figure 5. Block diagram of a ZP OFDM communication system. After [3].

Then, as discussed in [1], even and odd frequency components in the $2M$ DFT are related to each other. In fact, for any odd index k we can write

$$\sum_{\substack{l=0 \\ l \text{ even}}}^{2M-1} X_{2M}[l]W[k-l] + X_{2M}[k]W[0] = 0, \qquad (16)$$

where $w[n]$ is defined as

$$w[n]=\begin{cases}0 & \text{if } 0\le n\le M-1\\ 1 & \text{if } M\le n\le 2M-1\end{cases}, \tag{17}$$

and its $2M$ points FFT is defined as

$$W[k]=DFT\{w[n]\}. \tag{18}$$

The relation in (16) is due to the fact that

$$x[n]w[n]=0 \text{ for all } n=0,\ldots,2M-1, \tag{19}$$

and the DFT of the product is the circular convolution of the respective DFTs. The DFT of $w[n]$ can easily be computed as

$$W[k]=\sum_{n=M}^{2M-1} e^{-j\frac{2\pi}{2M}kn} \tag{20}$$

where

$$W[k]=0 \text{ for } k \text{ even} \tag{21}$$

and

$$W[0]=M. \tag{22}$$

Since in (16) l is even and k is odd, we let $k=2m+1$ with $m=0,...,M-1$ and, neglecting the noise term, rewrite (16) as

$$M\frac{Y[2m+1]}{C[2m+1]}=-\sum_{l=0}^{M-1}W[2(m-l)+1]X_M[l], \tag{23}$$

where $C[k], k=0,...,2M-1$ are the $2M$ points DFT of the channel's impulse response. We used the fact that the M point DFT of $x[n]$ corresponds to the even components of the zero padded $2M$ point DFT of $x[n]$.

Setting any given threshold, to be determined, we partition the transmitted data into two parts as

$$X[l] = X_{+}[l] + X_{-}[l], \tag{24}$$

with

$$X_{+}[l] = \begin{cases} X[l] \text{ if } |Y[2l]| > threshold \\ 0 \quad \text{if } |Y[2l]| \le threshold \end{cases} \tag{25}$$

and

$$X_{-}[l] = \begin{cases} X[l] \text{ if } |Y[2l]| \le threshold \\ 0 \quad \text{if } |Y[2l]| > threshold \end{cases}. \tag{26}$$

Now, we can write (23) as

$$\frac{Y[2m+1]}{C[2m+1]} = -\frac{1}{M}\sum_{l=0}^{M-1} W[2(m-l)+1]X_{+}[l] - \frac{1}{M}\sum_{l=0}^{M-1} W[2(m-l)+1]X_{-}[l]. \tag{27}$$

Define the following two M point IDFTs:

$$\begin{aligned} w_0[n] &= IDFT\{W[2k+1]\} = -e^{-j\frac{\pi}{M}n} \\ x_{\pm}[n] &= IDFT\{X_{\pm}[l]\} \end{aligned}. \tag{28}$$

Using the definitions in (27), we get

$$\frac{Y[2m+1]}{C[2m+1]} = -DFT\{w_0[n]x_{+}[n]\} - DFT\{w_0[n]x_{-}[n]\}. \tag{29}$$

If we take the inverse discrete Fourier transform (IDFT) and divide both sides by the term $w_0[n]$, we get

$$x_{-}[n] = -\frac{1}{w_0[n]} IDFT\left\{\frac{Y[2k+1]}{C[2k+1]}\right\} - x_{+}[n]. \tag{30}$$

Finally, the data recovered at, or close to, the nulls of the channel is

$$X_{\_}[l] = DFT\{x_{\_}[n]\}, l = 0,...,M-1. \tag{31}$$

Thus, (31) shows that we can recover data transmitted through subcarriers with zero or close to zero frequency response of the channel [1]. However, this algorithm can be fairly sensitive to noise, and in the next section, we present an improvement based on Kalman filtering estimation.

B. OPTIMAL ESTIMATION ALGORITHM

In this section, we recall some of the relevant results in linear optimal estimation. These results are at the base of the Kalman filter, which provides the main equations in the optimal estimator. In particular, consider the case where we want to estimate a random vector $\underline{X}$ based on an observation vector $\tilde{\underline{Y}}$ linearly related to $\underline{X}$ as

$$\tilde{\underline{Y}} = \bar{C}\underline{X} + \underline{V} \tag{32}$$

where $\underline{V}$ represents random noise with zero mean and covariance R, independent of $\underline{X}$. Also, we have a priori knowledge of the vector $\underline{X}$ in terms of its expected value

$$\hat{\underline{X}}_0 = E\{\underline{X}\} \tag{33}$$

and its covariance matrix

$$P_0 = E\left\{\left(\underline{X} - \hat{\underline{X}}_0\right)\left(\underline{X} - \hat{\underline{X}}_0\right)^H\right\}. \tag{34}$$

Now, from (32) it is known that the optimal linear estimator for $\underline{X}$ is of the form [5]

$$\hat{\underline{X}} = \hat{\underline{X}}_0 + K(\tilde{\underline{Y}} - \bar{C}\hat{\underline{X}}_0) \tag{35}$$

where

$$K = P_O\bar{C}^H\left(R + \bar{C}P_O\bar{C}^H\right)^{-1} \tag{36}$$

is called the Kalman gain.

If we define the covariance matrix

$$P = E\left\{\left(\underline{X} - \underline{\hat{X}}\right)\left(\underline{X} - \underline{\hat{X}}\right)^H\right\}, \tag{37}$$

then we can compute the covariance of the estimate as

$$P = P_0 - P_0\overline{C}^H\left(R + \overline{C}P_0\overline{C}^H\right)\overline{C}P_0. \tag{38}$$

For this thesis we need to estimate $X_-[l_i], i = 1,...,k_{low},$ which is the data associated with the carriers with SNR below a certain threshold. Although this can be applied to any signal constellation, we assume for simplicity that each $X[k]$ has a QPSK sequence with zero mean and unit power. In order to determine the observation vector $\underline{\tilde{Y}}$, we combine the received signal $y[n]$ with $n = 0,\ldots,P-1$ and its $2M$ point DFT as

$$Y[k] = DFT\{y[n]\},\ k = 0,\ldots,2m-1. \tag{39}$$

Given that the data $X_+[k]$ from the subcarriers with high SNR can be demodulated with very low probability of error, from (27) we have

$$\begin{aligned} Y[2m+1] + \frac{C[2m+1]}{M}\sum_{l=0}^{M-1} W\left[2(m-l)+1\right]X_+[l] = \\ -\frac{C[2m+1]}{M}\sum_{l=0}^{M-1} W\left[2(m-l)+1\right]X_-[l] + V\left[2(m+1)\right] \end{aligned}. \tag{40}$$

The a priori information on $X_-[k]$ is based on the fact that, for both BPSK with $X = \{-1,+1\}$ and QPSK where $X = \left\{\pm 1/\sqrt{2} \pm j\ 1/\sqrt{2}\right\},$ the mean is given by

$$\hat{X}_0 = E\{X\} = 0 \tag{41}$$

and the covariance

$$E\left\{\left(X-\hat{X}_0\right)^2\right\}=E\left\{\left|X\right|^2\right\}=1. \tag{42}$$

Assuming that all the data samples $X[k]$ are independent of each other, we see that the covariance matrix is diagonal with unit values, which leads to

$$P_0=I. \tag{43}$$

For the noise, since the received data block has length $P=M+L$, the corresponding noise term $v[n]$ with $n=0,\ldots,P-1$ is assumed to be white with zero mean and covariance

$$E\left\{\left|v[n]\right|^2\right\}=\sigma^2. \tag{44}$$

Therefore, the $2M$ point DFT is defined as

$$V[k]=\sum_{n-0}^{P-1}v[n]e^{-j\frac{2\pi}{2M}kn},k=0,\ldots,2M-1, \tag{45}$$

which leads to the covariance matrix expression for the noise vector $V[k]$ with $n=0,\ldots,2M-1$ in every block as

$$\begin{aligned}&R[l]=E\left\{V[k]V^*[k-l]\right\}=\\&E\left\{\left(\sum_{n_1=0}^{P-1}v[n_1]e^{-j\frac{2\pi}{2M}kn_1}\right)\left(\sum_{n_2=0}^{P-1}v^*[n_2]e^{j\frac{2\pi}{2M}(k-l)n_2}\right)\right\}=\\&\sum_{n_1}^{P-1}\sum_{n_2}^{P-1}E\left\{v[n_1]v^*[n_2]\right\}e^{-j\frac{2\pi}{2M}kn_1}e^{j\frac{2\pi}{2M}(k-l)n_2}=\\&\sigma^2\sum_{n=0}^{P-1}e^{-j\frac{2\pi}{2M}kn}e^{j\frac{2\pi}{2M}(k-l)n}=\sigma^2\sum_{n=0}^{P-1}e^{-j\frac{\pi}{M}ln}\end{aligned}. \tag{46}$$

Applying the geometric series outcome to the last equation in (46) leads to

$$R[l] = \sigma^2 \frac{1 - e^{-j\frac{\pi}{M}Pl}}{1 - e^{-j\frac{\pi}{M}l}}, \quad l = 0, \ldots, 2M-1. \tag{47}$$

Since (32) and (40) involve only odd frequency terms, we obtain the covariance matrix expression as

$$R = E\left\{VV^{*T}\right\} = E\left\{\begin{vmatrix} V[1] \\ \vdots \\ V[2M-1] \end{vmatrix} \begin{vmatrix} V[1] & V[3] & \cdots & V[2M-1] \end{vmatrix}\right\} =$$

$$\begin{vmatrix} R[0] & R[2] & \cdots & R[2M-2] \\ \vdots & \ddots & \ddots & \vdots \\ \vdots & \ddots & \ddots & \vdots \\ R[2M-2] & \cdots & \cdots & R[0] \end{vmatrix} . \tag{48}$$

From (35), (36), (41) and (43), we get

$$\underline{\hat{X}} = K\underline{\tilde{Y}} \tag{49}$$

where

$$K = \bar{C}^H \left(R + \bar{C}\bar{C}^H\right)^{-1}. \tag{50}$$

In (49), $\underline{\hat{X}}$ is the estimate of $X_{-}[l_i]$, the vector of subcarriers with SNR lower than the threshold, and $\underline{\tilde{Y}}$ is the information that we observe. Specifically, the observation vector, involving the received signal and the demodulated subcarriers with high SNR, is defined as

$$\underline{\tilde{Y}} = \left[\tilde{Y}[0], \ldots, \tilde{Y}[M-1]\right]^T, \tag{51}$$

where

$$\tilde{Y}[m] = Y[2m+1] + \frac{C[2m+1]}{M} \sum_{l=0}^{M-1} W\left[2(m-l)+1\right] X_{+}[l]. \tag{52}$$

Note that the matrix $\bar{C}$ included in (50) is an expression depending on indices m and i, where $m = 0,...,M-1$ and i are the indices of the data associated to the carriers with SNR below a certain threshold.

Specifically, we can define the matrix $\bar{C}[m,i]$ as

$$\bar{C}[m,i] = -\frac{C[2m+1]}{M} W[2(m-l_i)+1] \tag{53}$$

where $m = 0,...,M-1$ and i is the index of the data associated with low SNR subcarriers. The length l_i is k_{low}. Eventually, this will lead to a matrix $\bar{C}[m,i]$ of dimensions $M \times k_{low}$.

In the Kalman gain defined in (50), the matrix $\bar{C}$, has many more rows than columns. As a consequence, the dimension of $\bar{C}\bar{C}^H$ is much larger than the dimension of $\bar{C}^H\bar{C}$.

As will be explained below, (50) can also be rewritten as

$$\bar{C}^H\left(R+\bar{C}\bar{C}^H\right)^{-1} = \left(I+\bar{C}^H R^{-1}\bar{C}\right)^{-1}\bar{C}^H R^{-1} \tag{54}$$

where the inverse matrix expression present in the right hand side of the expression has a much lower dimension than the inverse matrix expression present in the left hand side of the expression.

In order to see this, notice that for any matrix $\bar{C}$ we have

$$\bar{C}^H(I+\bar{C}\bar{C}^H)^{-1} = (I+\bar{C}^H\bar{C})^{-1}\bar{C}^H. \tag{55}$$

This result follows from the identity

$$\begin{aligned}&(I+\bar{C}^H\bar{C})C^H(I+\bar{C}^H\bar{C})^{-1} = (\bar{C}^H+\bar{C}^H\bar{C}\bar{C}^H)(I+\bar{C}^H\bar{C})^{-1} = \\ &\bar{C}^H(I+\bar{C}\bar{C}^H)(I+\bar{C}^H\bar{C})^{-1} = \bar{C}^H\end{aligned}. \tag{56}$$

Now, any positive definite matrix R can be written as the product

$$R = Q^H Q. \tag{57}$$

So, now we have

$$\begin{aligned} &\bar{C}^H (I + \bar{C}\bar{C}^H)^{-1} = \bar{C}^H (Q^H Q + \bar{C}\bar{C}^H)^{-1} = \\ &\bar{C}^H (Q\left(I + \left(Q^H\right)^{-1} \bar{C}\bar{C}^H Q^{-1}\right)Q)^{-1} = \\ &\bar{C}^H Q^{-1}\left(I + \left(Q^H\right)^{-1} \bar{C}\bar{C}^H Q^{-1}\right)\left(Q^H\right)^{-1} \end{aligned} . \tag{58}$$

Applying this result to formula (54), we get

$$\left(I + \bar{C}^H Q^{-1}\left(Q^H\right)^{-1} \bar{C}\right)^{-1} \bar{C}^H Q^{-1}\left(Q^H\right)^{-1}. \tag{59}$$

Finally, we get

$$\bar{C}^H \left(R + \bar{C}\bar{C}^H\right)^{-1} = \left(I + \bar{C}^H R^{-1}\bar{C}\right)^{-1} \bar{C}^H R^{-1} \tag{60}$$

which is the desired equality.

C. SUMMARY OF THE PROPOSED OPTIMAL ALGORITHM

A summary of the algorithm steps is given here. Let M and L be the lengths of the FFT and the prefix. Also, let $C[k], k = 0,...,2M-1$ be the $2M$ point FFT and the channel impulse response. Then:

Step 1: Given each received OFDM symbol $y[n],\ n = 0,\ldots,M+L-1,$ compute its zero padded $2M$ point FFT $Y[k] = FFT\{y[n], n = 0,...,2M-1\}$.

Step 2: Partition the indices $k = 0,...,M-1$ into k_+ and k_- according to the expression

$$\begin{aligned} &\left|Y[2k_+]\right| > threshold \\ &\left|Y[2k_-]\right| < threshold \end{aligned} .$$

Step 3: Demodulate the subcarriers labeled by k_+ (the ones with high SNR) as

$$X\left[k_+\right] = MQAM\left\{\frac{Y[2k_+]}{C[2k_+]}\right\}.$$

Step 4: Form the matrix $\bar{C}\left[m,i\right] = -\frac{C\left[2m+1\right]}{M} W\left[2\left(m-l_i\right)+1\right].$

Step 5: Form the observation vector $\underline{\tilde{Y}}$ as $\underline{\tilde{Y}} = \left[\tilde{Y}\left[0\right],\ldots,\tilde{Y}\left[M-1\right]\right]^T$.

Step 6: For each subcarrier k_- with low SNR, let $\underline{\hat{X}}\left[k_-\right] = K\underline{\tilde{Y}}$ with $K = \left(I + \bar{C}^H R^{-1} \bar{C}\right)^{-1} \bar{C}^H R^{-1}.$

Step 7: Demodulate the subcarriers with low SNR as

$$\underline{X}\left[k_-\right] = MQAM\left\{\underline{\hat{X}}[k_-]\right\}.$$

THIS PAGE INTENTIONALLY LEFT BLANK

IV. IEEE 802.11 OFDM IMPLEMENTATION

In this work, we do not include nulls or pilots in the OFDM symbols as is the case of the OFDM symbol format described in the IEEE Standard 802.11a. This choice was made to test the proposed concept of null estimation without having to worry about the effects of the nulls in the OFDM symbol. In addition, we assume full knowledge of the channel characteristics.

Three sets of simulations were conducted. First, a fading noisy channel was used for a QPSK signal. We used random channels, all with zero frequency response at a specific random frequency ω_0, changing for every block of data. This condition was selected to simulate a continuous random fading channel. The threshold was set in terms of the SNR of each single subcarrier so that by setting $thresh\_dB = 10$ dB (say) all received subcarriers above (below) the threshold have an SNR larger (smaller) than 10 dB. This condition was selected to compare the efficiency of the proposed optimal estimator to that of the standard OFDM receiver algorithm. The same simulation was also conducted using SIMULINK for real-time implementation.

The second set of simulations investigated the identification of the optimal threshold. Here, the goal was to identify a threshold value that leads to the smallest symbol error rate (SER). For simplicity, we also used random channels, all with zero frequency response at a specific frequency ω_0. Results showed that for specific $\mathrm{SNR}_{\mathrm{dB}}$, a different threshold should be used for best performance.

The third set of simulations investigated PAPR clipping and its effect on the SER and compared results to those obtained with the standard OFDM receiver algorithm. The PAPR values used for the simulations were 5 dB, 6 dB and 7 dB, in the sense that all signal values larger than the sum of the standard deviation value of the signal plus the PAPR level, in dB, are clipped. A noisy, non-deep fading channel was used in this scenario. This modification does not affect the generality of the results.

A. EFFICIENCY OF THE KALMAN FILTER ALGORITHM

For testing, we used random channels, all with zero frequency response at a random frequency ω_0. A snapshot of the channel frequency response is shown in Figure 6. We can see a situation in which the information at subcarrier ω_0 is completely lost even at very high SNR.

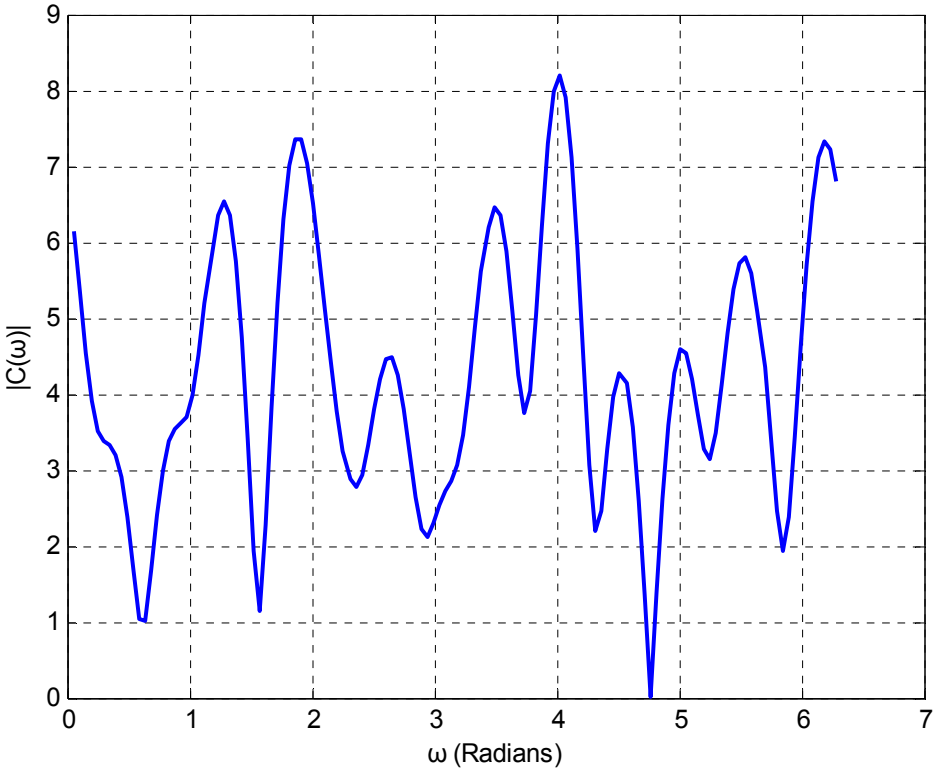

Figure 6. Channel frequency response with null at a random frequency ω.

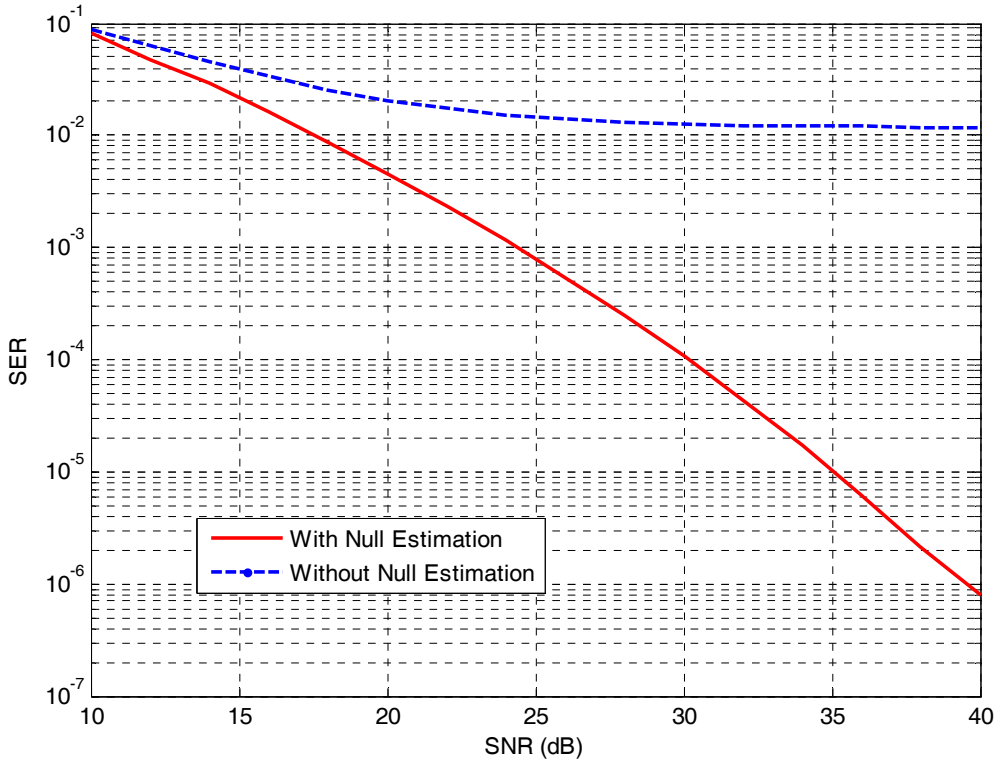

Figure 7. Comparison of the IEEE 802.11 standard QPSK symbol error rate between a standard OFDM receiver algorithm and an optimal estimation (based on the Kalman filter) OFDM receiver algorithm.

The performance of the standard algorithm (dashed line) is compared with that of the proposed algorithm (solid line) in terms of SER versus SNR in Figure 7. The proposed optimal OFDM receiver algorithm performs as expected. It is noticeable that above 25 dB the standard OFDM receiver algorithm remains constant at 11.8×10^{-3} SER due to the information lost in the deep faded subcarriers, where the channel frequency response has a null, but the proposed algorithm is able to recover the data, improving the SER.

A QPSK signal transmitted through a noisy channel was simulated in SIMULINK to test a real-time implementation. We used random channels, all with zero frequency response at a predefined random frequency ω_0. The random frequency ω_0 was selected

and kept constant throughout the simulation. Results showed that the SER obtained with the SIMULINK simulation matched those obtained with the MATLAB implementation.

B. THRESHOLD IDENTIFICATION

For simplicity, in this case we used channels, all with zero frequency response at a specific fixed frequency ω_0. An example of channel frequency response is shown in Figure 8.

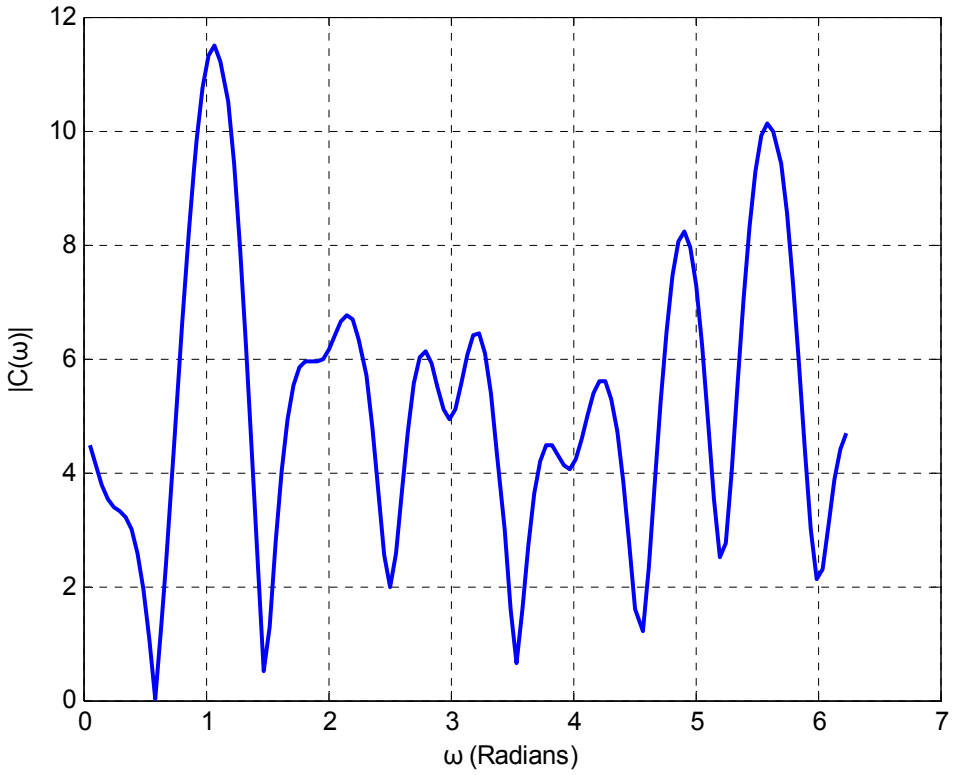

Figure 8. Channel frequency response with null at $\omega = 0.589$ radians.

In order for the optimal threshold value to be identified, tests were conducted for a specific $\mathrm{SNR}_{\mathrm{dB}}$ and a range of thresholds. Tests showed that the optimal threshold is dependent on the signal SNR.

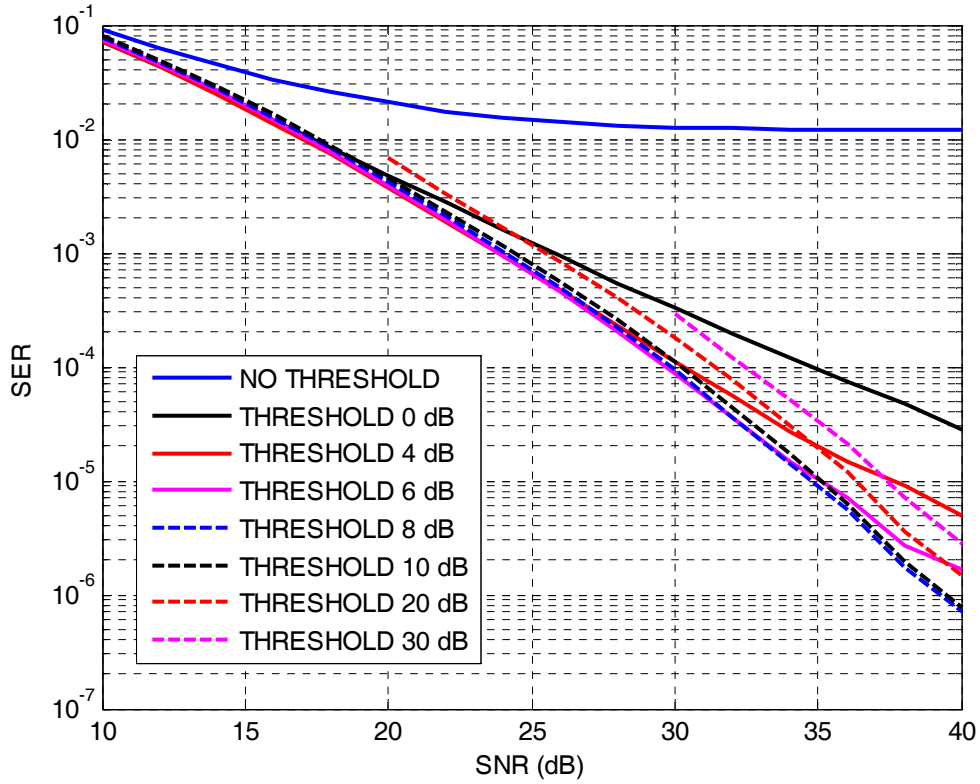

Figure 9. Comparison of the IEEE 802.11 standard QPSK SER between different threshold values for optimal estimation (based on the Kalman Filter) OFDM receiver algorithm.

In Figure 9, SER values for different threshold values used with the optimal estimation OFDM receiver algorithm are presented. It can be seen that the best SER results are achieved for different threshold depending on SNR_{dB}.

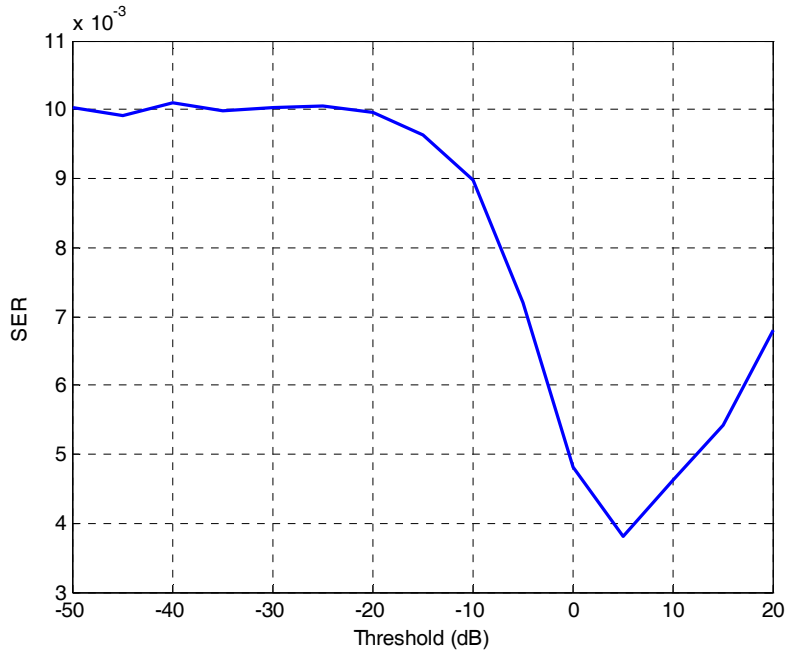

Figure 10. QPSK symbol error rate for SNR = 20 dB and threshold values for a range between -50 dB to 20 dB.

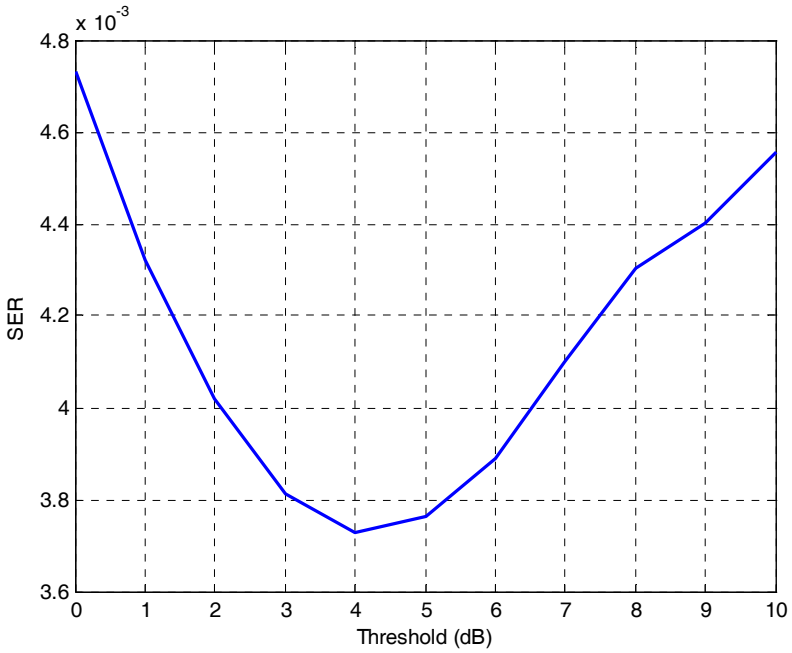

Figure 11. QPSK symbol error rate for SNR = 20 dB and threshold values for a range between 0 dB to 10 dB.

The case of $SNR_{dB} = 20\,dB$ and a threshold range between -50 dB to 20 dB is illustrated in Figure 10. We notice that the best results are obtained around a $5\,dB$ threshold value. In Figure 11, results obtained for $SNR_{dB} = 20\,dB$ and a threshold range from $0\,dB$ to $10\,dB$ are presented. Results show the best performance is obtained for a threshold value equal to $4\,dB$.

Table 2. Optimal threshold values for specific SNR_{dB} values.

$Threshold_{dB}$	4	5	6	7	8
SNR_{dB}	15-19	20-24	25-30	31-35	36-40

In Table 2, optimal threshold values obtained for specific SNR_{dB} values are shown. We conclude that we must adjust the threshold depending on the SNR_{dB} in order to get best SER results.

C. PEAK-TO-AVERAGE POWER RATIO

1. Introduction

An OFDM signal consists of a number of independently modulated subcarriers. These subcarriers when added up coherently can lead to a large peak-to-average power ratio. Moreover, they produce a peak value that can be up to N times the root mean square (RMS) value when N signals are added with the same phase [6].

A large PAPR is a drawback inherent in OFDM signals. For example, the complexity of the analog-to-digital and digital-to-analog converters is increased and the efficiency of the radio frequency (RF) power amplifier is reduced.

Several techniques have been proposed to reduce the PAPR. The first category of techniques consists of signal distortion techniques, which reduce the peak amplitudes nonlinearly, distorting the OFDM signal at or around the peaks. These techniques include

clipping, peak windowing and peak cancellation. The second category involves coding techniques that use a forward-error correction code set that excludes OFDM symbols with a large PAPR. The third category is based on scrambling each OFDM symbol with different scrambling sequences and selecting that sequence that gives the smallest PAPR [6].

In this work, we reduce the PAPR by clipping the peaks.

2. Clipping

The simplest approach to reduce the PAPR is to clip the signal, which results in limiting the peak amplitude to some desired maximum level. Although clipping is the simplest solution, there are a few problems associated such as self-interference and SER degradation. Moreover, the nonlinear distortion of the OFDM signal increases the level of the out-of-band radiation [6].

For the MATLAB implementation and simulations, the signal standard deviation was taken as the reference value. From this point, the desired PAPR in dB is the quantity which defines the maximum allowed peak. The formula used is

$$\max_{peak} = \sigma_x \cdot 10^{(PAPR_{dB}/20)}, \tag{61}$$

where σ_x is the standard deviation of the signal.

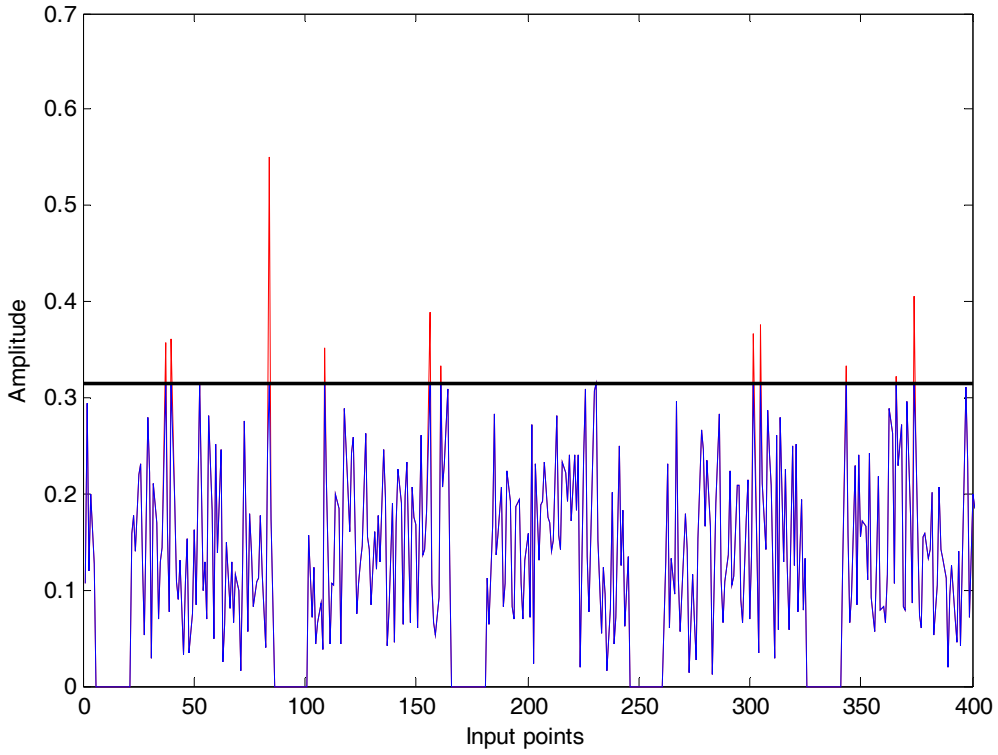

Figure 12. Signal before and after clipping.

In Figure 12, 400 points of the input data are illustrated. The clipping was performed for $PAPR_{dB} = 6$ dB based on (61).

For the simulation, a noisy non-deep fading channel was selected and a QPSK signal generated for a range of $\mathrm{SNR}_{\mathrm{dB}}$ values between 20 dB to 30 dB.

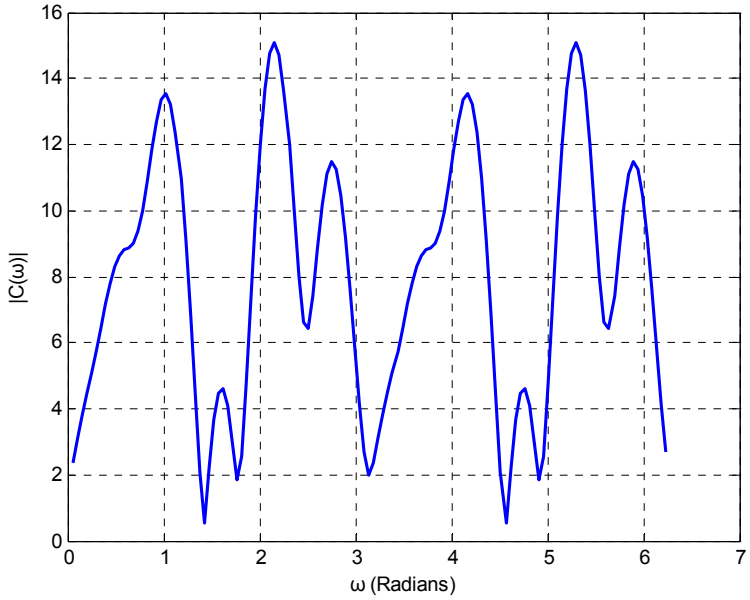

Figure 13. Frequency response of the channel used for the simulation.

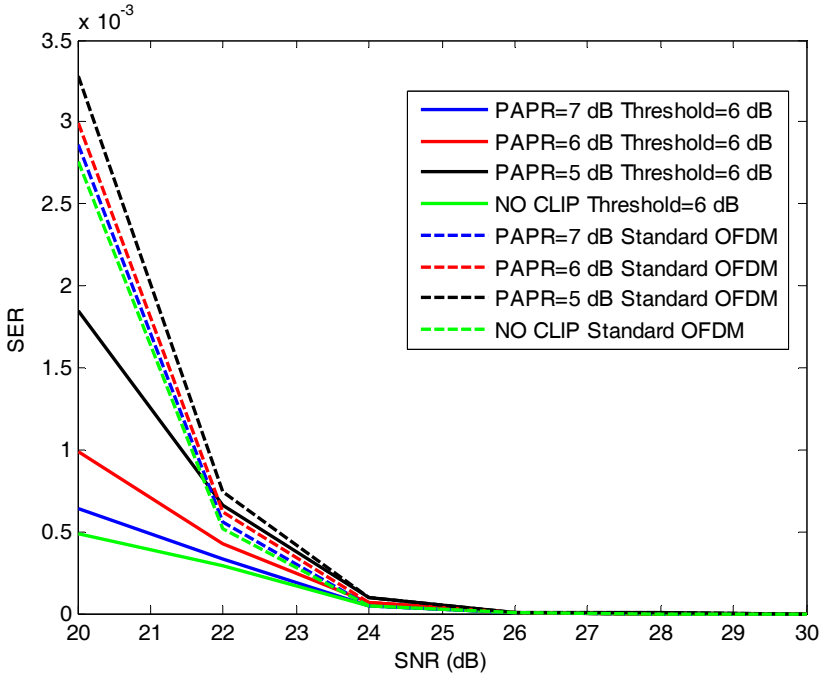

Figure 14. Comparison of the IEEE 802.11 standard QPSK SER with a standard OFDM receiver algorithm and optimal estimation (based on the Kalman filter) OFDM receiver algorithm for different cases of PAPR clipping.

In Figure 13, results obtained with this scheme are illustrated. The performance of the standard algorithm (dashed line) is compared with that of the proposed algorithm (solid line) in terms of symbol error rate versus SNR for different values of PAPR in dB. Specifically, the values that were chosen for the maximum clipped PAPR were 5 dB, 6 dB and 7 dB. Note that a larger SER results when the clipping increases. Results show that the proposed optimal algorithm overall performs better since its SER is lower than that obtained with a standard OFDM receiver algorithm for all SNRs investigated.

THIS PAGE INTENTIONALLY LEFT BLANK

V. IEEE 802.16 OFDM IMPLEMENTATION

In previous chapters, we developed an OFDM ZP receiver to recover data from channels with nulls at one or more frequencies. Channels used for testing were sort of extreme in the sense that they have absolute nulls at one or more frequencies.

More realistic channels have less severe constraints. Their frequency responses might attenuate some frequencies, but in general, every subcarrier carries information. In this section we test whether the added complexity of the proposed algorithm is of any benefit in less severe and more realistic situations.

In what follows, testing was extended to include the case of an OFDM signal based on the 802.16 IEEE Standard. This specific configuration was chosen since a number of standard channels describing different environments are widely available.

As investigated in the IEEE 802.11 standard scenario, we first identify an optimal value for the threshold and then test the proposed scheme on different channels.

A. THRESHOLD IDENTIFICATION

For this thesis, we generated a signal with $M = 256$ data sub-carriers and a zero prefix of length $L = 32$.

First, we identified the optimal threshold value. For the case of the 802.16 OFDM signal, we chose SNRs in the range between 20 and 30 dB. Results obtained for SNR equal to 26 dB are presented in Figure 15 and Figure 16.

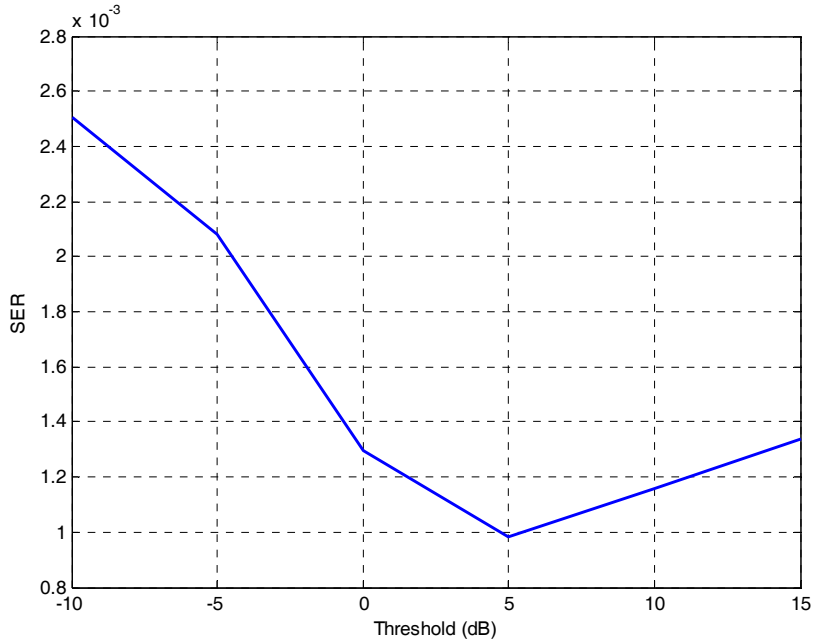

Figure 15. QPSK symbol error rates for SNR = 26 dB and threshold values for a range between -10 dB to 15 dB.

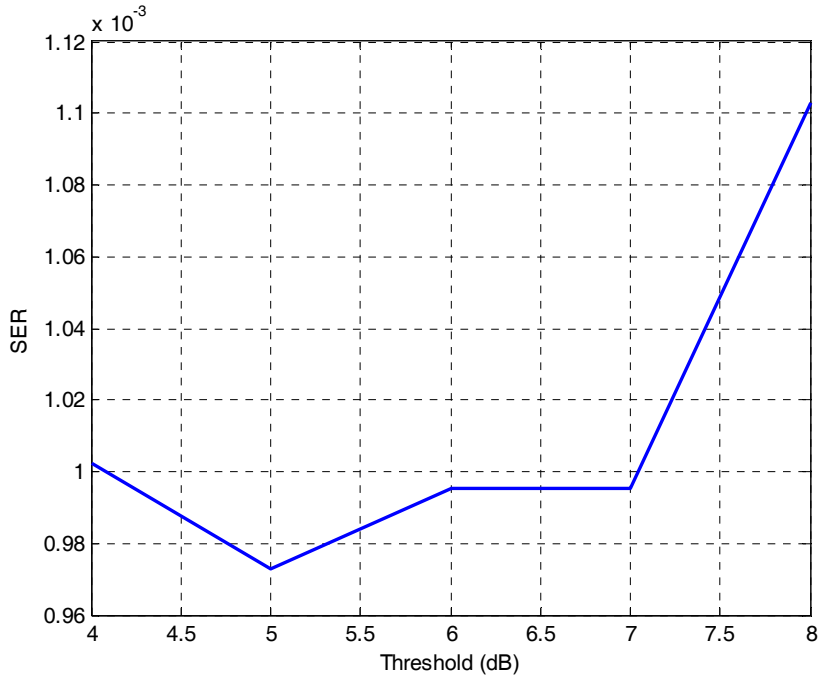

Figure 16. QPSK symbol error rates for SNR = 26 dB and threshold values for a range between 4 dB to 8 dB.

From the results, we can see that the best performances are obtained around a 5 dB threshold value. In Figure 16 results obtained for $\mathrm{SNR}_{\mathrm{dB}} = 26\,\mathrm{dB}$ and a threshold range between 4 dB to 8 dB are shown. In this case, best results are achieved for the value of 5 dB.

B. EFFICIENCY OF THE KALMAN FILTER ALGORITHM

The next phase compares the efficiency of the optimal estimation algorithm to that of the standard OFDM receiver algorithm. Two simulations were conducted, the first used random channels, all with zero frequency response at a random frequency ω_0 changing for every block of data, and the second used random channels, all with zero frequency response at a specific frequency ω_0.

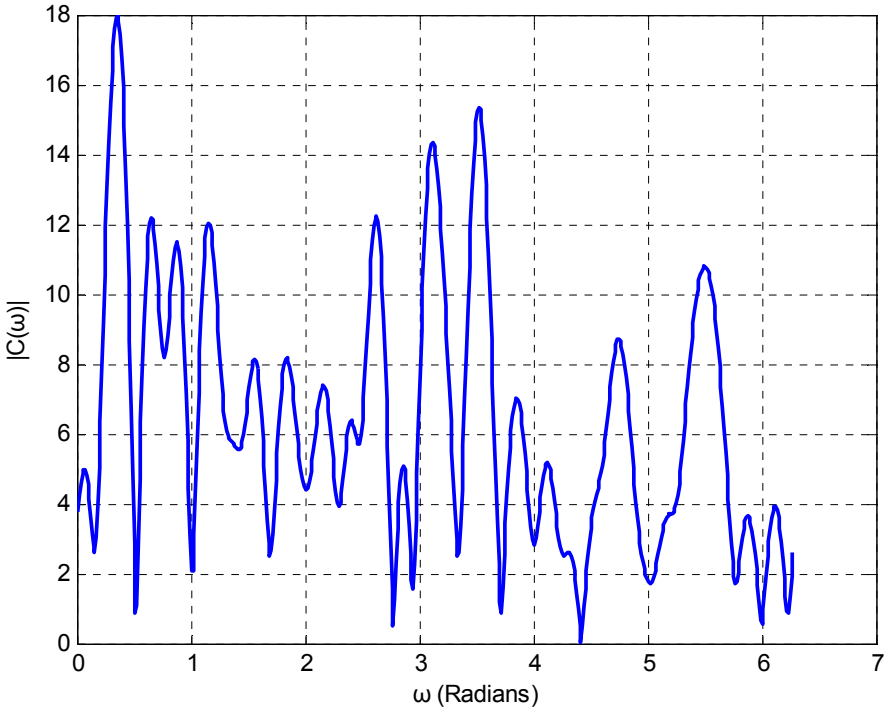

Figure 17. Channel frequency response with null at a random frequency ω_0.

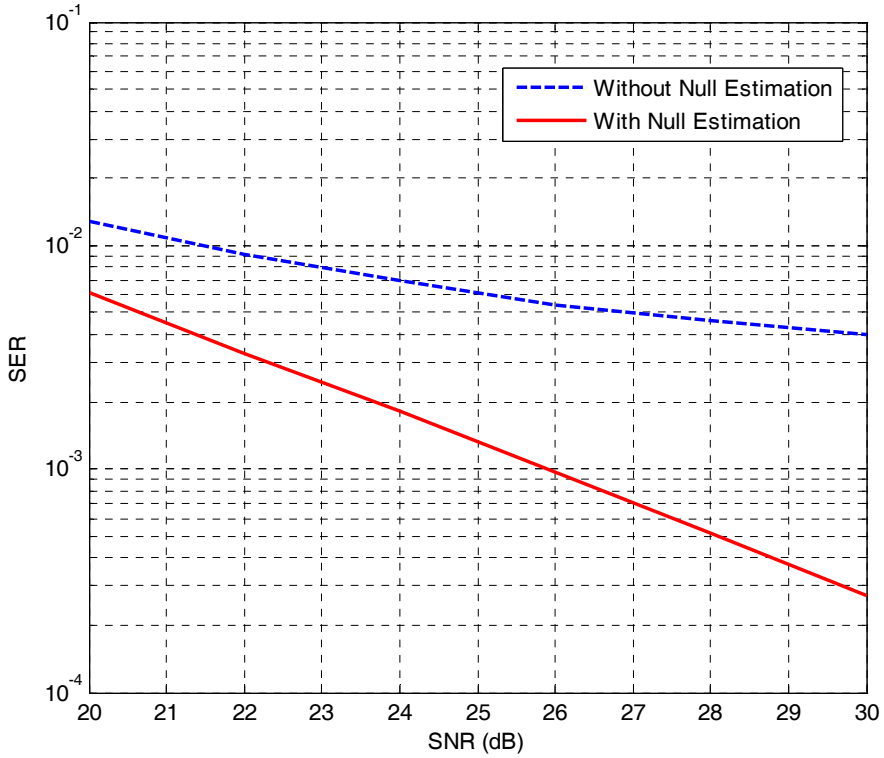

Figure 18. Comparison of the 802.16 standard QPSK SER with a standard OFDM receiver algorithm and optimal estimation (based on the Kalman filter) OFDM receiver algorithm.

In Figure 17, a snapshot of the channel frequency response is shown. The performance of the standard algorithm (dashed line) is compared with that of the proposed algorithm (solid line) in terms of symbol error rate versus SNR, and the results are presented in Figure 18. Results show that the optimal estimation OFDM receiver algorithm performs better than the standard OFDM receiver algorithm.

In Figure 19, a snapshot of a channel frequency response, with null at $\omega = 0.589$ radians is shown. The QPSK symbol error rate values obtained for SNR values between 20 dB to 30 dB for the standard OFDM receiver algorithm and the optimal estimation (based on the Kalman filter) OFDM receiver algorithm are presented in Figure 20. We conclude that the optimal estimation OFDM receiver algorithm performs better than the standard OFDM receiver algorithm.

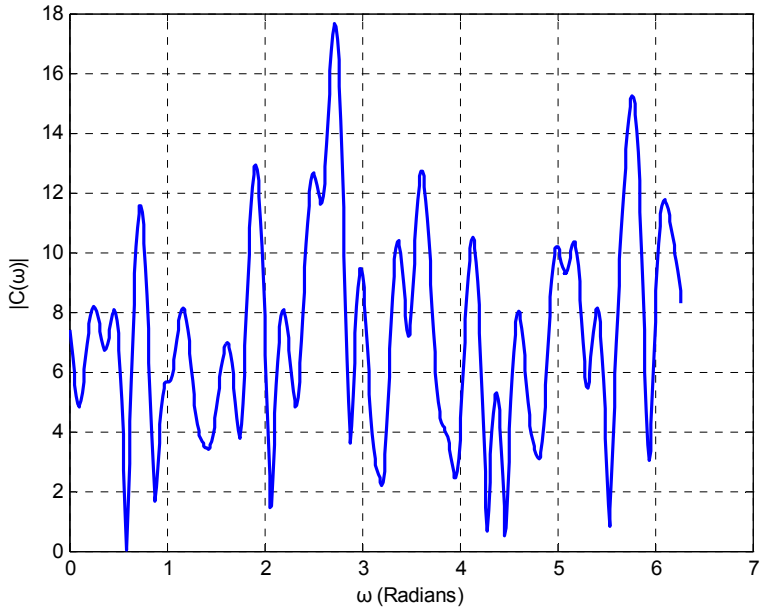

Figure 19. Channel frequency response with null at $\omega = 0.589$ radians.

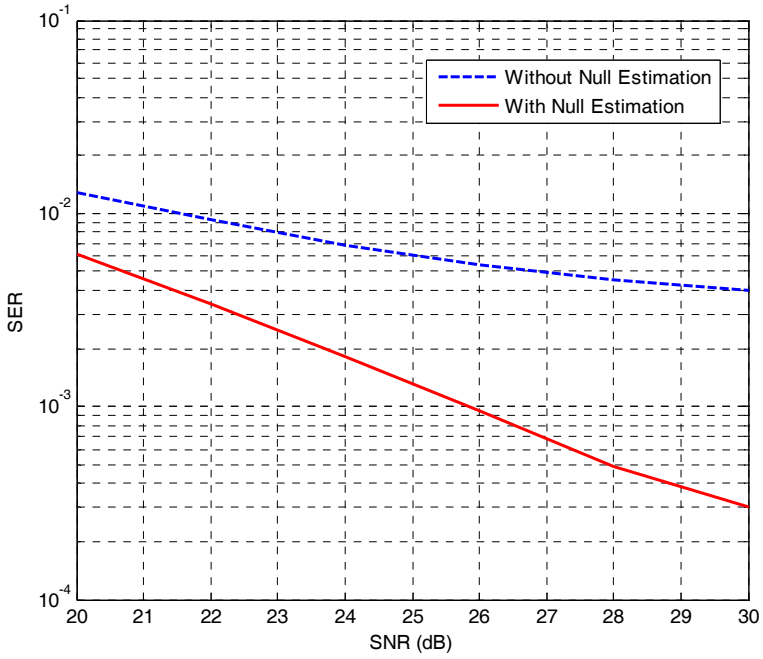

Figure 20. Comparison of the IEEE 802.16 standard QPSK SER with a standard OFDM receiver algorithm and optimal estimation (based on the Kalman filter) OFDM receiver algorithm.

C. PEAK-TO-AVERAGE POWER RATIO CLIPPING

In this simulation phase, we use a noisy non-deep fading channel and a QPSK signal for a range of SNR_{dB} values from 20 dB to 30 dB. The channel model was identical to that selected in the 802.11 OFDM signal case considered earlier.

The results are illustrated in Figure 21.

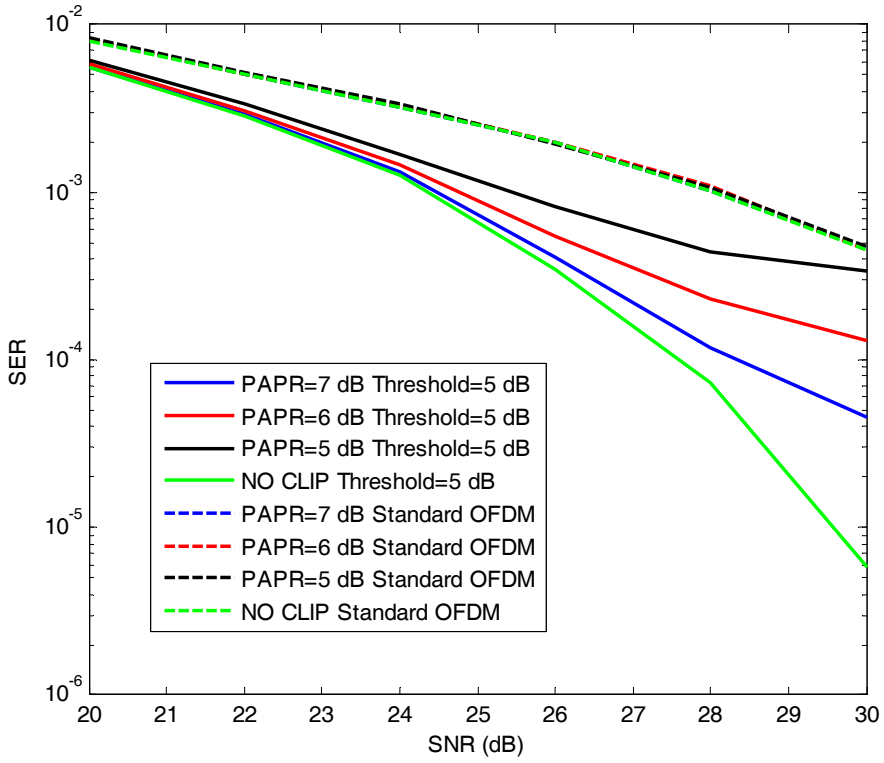

Figure 21. Comparison of the IEEE 802.16 standard QPSK SER with a standard OFDM receiver algorithm and optimal estimation (based on the Kalman filter) OFDM receiver algorithm for different cases of PAPR clipping.

The performance of the standard algorithm (dashed line) is compared to that of the proposed algorithm (solid line) in terms of SER versus SNR, for different values of PAPR in dB. The values that were chosen are 5 dB, 6 dB and 7 dB. Note that the errors increase with clipping level. Results show that the proposed optimal algorithm overall performs better. In addition, they show that the symbol error rate is still lower

when using the proposed scheme and clipping is applied to reduce the PAPR effect than when using the standard OFDM receiver algorithm.

D. STANFORD UNIVERSITY INTERIM (SUI) CHANNELS

In this section, we test the algorithm for more realistic channels. In particular, there are six channel models that represent three terrain types. They also represent various Doppler spreads, delay spread and line-of-sight (LOS) / non-line-of-sight (NOLOS) conditions that are typical of the continental United States. These models can be used for simulations, design, development, and testing of technologies suitable for fixed broadband wireless applications [7].

As we see in Table 3, the maximum path loss category is the hilly terrain with moderate-to-heavy tree densities (Category A). The intermediate path loss condition is referred as Category B. The minimum path loss category is mostly flat terrain with light tree densities (Category C) [7].

Table 3. Terrain type and Doppler spread for SUI channel models. From [7].

Channel	Terrain Type	Doppler Spread	Spread	LOS
SUI-1	C	Low	Low	High
SUI-2	C	Low	Low	High
SUI-3	B	Low	Low	Low
SUI-4	B	High	Moderate	Low
SUI-5	A	Low	High	Low
SUI-6	A	High	High	Low

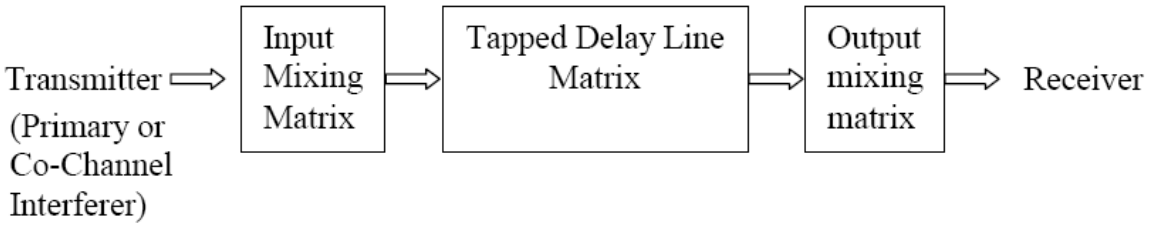

Figure 22. Generic structure of SUI channel models. From [7].

The generic structure for the SUI channel model is shown in Figure 22. This structure is applicable for multiple-input-multiple-output (MIMO) channels. It also includes configurations to accommodate the single-input-single-output (SISO) and single-input-multiple-output (SIMO) cases. The SUI channel structure is the same for the primary and interfering signals. Multipath fading is modeled for each channel as a tapped-delay line with three taps with non-uniform delays. A distribution (Ricean with a K-factor > 0 or Rayleigh with K-factor = 0) and the maximum Doppler frequency characterizes the gain associated with each tap [8].

Using the general structure from Figure 22 and assuming the scenario from Table 4, we simulated a set of six SUI channels, which are representative of real-world channels.

Table 4. Scenario for SUI channel models. From [8].

Cell size	7 km
BTS Antenna Height	30 m
Receive Antenna Height	6 m
BTS Antenna beam Width	120°
Receive Antenna Beam Width	Omni directional (360°) and 30°.
Vertical Polarization Only	
90% cell coverage with 99.9% reliability at each location covered.	

1. SUI-3 Channel Implementation

For this part of the thesis, we selected a SUI-3 omni antenna channel based on [6] and tested the OFDM signal based on the 802.16 algorithm.

In Figure 23, a snapshot of the SUI-3 channel frequency response is shown.

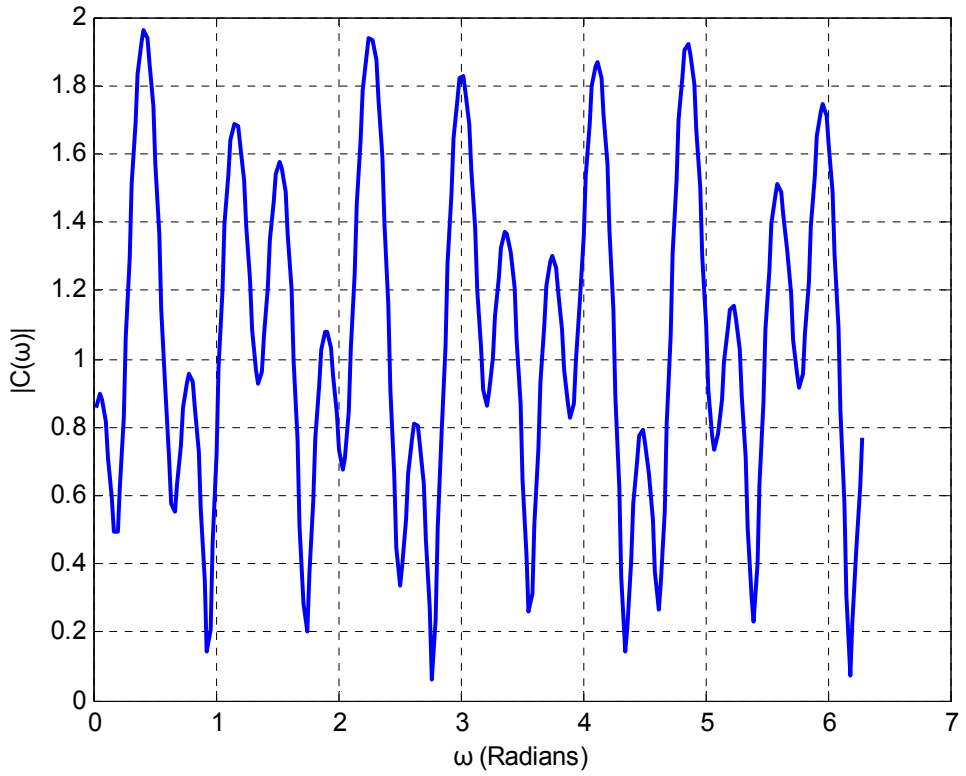

Figure 23. Snapshot of the SUI-3 channel frequency response used for the simulation.

As previously, we initially identify the optimal threshold value by simulation. In Figure 24, results obtained for SNRs of 14 dB, 20 dB and 26 dB are illustrated. Results show that the optimal threshold value is around 6 dB. Further simulations showed the best SER value is obtained when the threshold is between 4 dB and 8 dB. Thus, we used a threshold of 6 dB in this set of simulations.

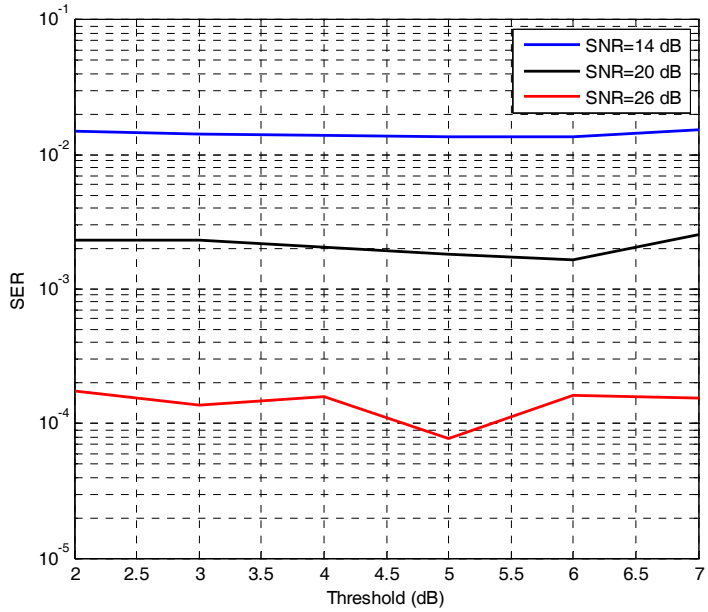

Figure 24. QPSK symbol error rates for SNR values of 14 dB, 20 dB and 26 dB and threshold values for a range between 2 dB to 7 dB.

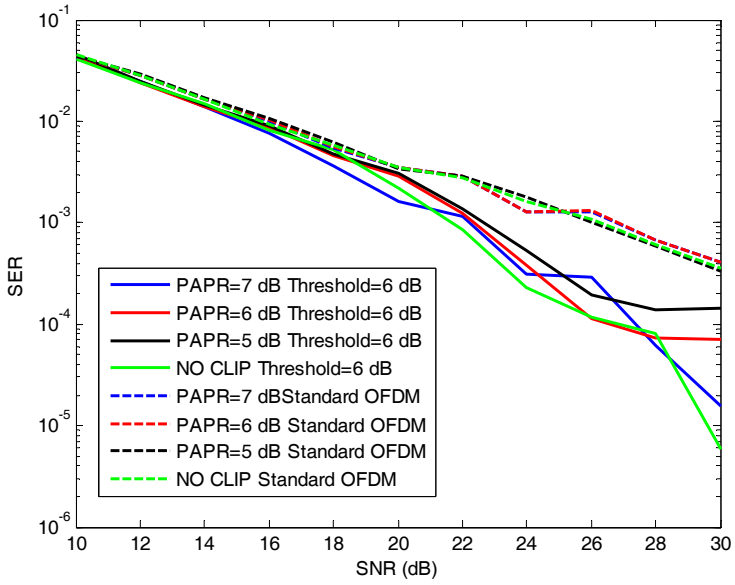

Figure 25. Comparison of the IEEE 802.16 standard QPSK SER with a standard OFDM receiver algorithm and optimal estimation (based on the Kalman filter) OFDM receiver algorithm for different cases of PAPR clipping for a SUI-3 channel.

Next, we tested the optimal estimation algorithm and compared it with the standard OFDM receiver algorithm for various PAPR clipping conditions. The results of these simulations are shown in Figure 25.

The performance of the standard algorithm (dashed line) is compared with that of the proposed algorithm (solid line) in terms of symbol error rate versus SNR for different values of PAPR in dB. The values chosen are again 5 dB, 6 dB and 7 dB. Results show that the proposed Kalman-based optimal algorithm overall performs better than the standard OFDM receiver algorithm for every condition considered.

2. Non-Line-of-Sight Condition Implementation

The SUI-3 channel implemented has some LOS characteristics and low spread, as we can see from Table 3. To test the efficiency of the optimal estimation algorithm, we modified the SUI-3 channel in this phase by changing the K-factor in order to generate a NOLOS fading channel. This modification did not affect the quality of the results of our simulations. This simulation is an introduction to SUI-4, SUI-5 and SUI-6 channel testing for which the optimal estimation algorithm has to be modified further.

The testing conditions and parameters were the same as those selected for the SUI-3 channel case.

A snapshot of the modified SUI-3 channel is illustrated in Figure 26.

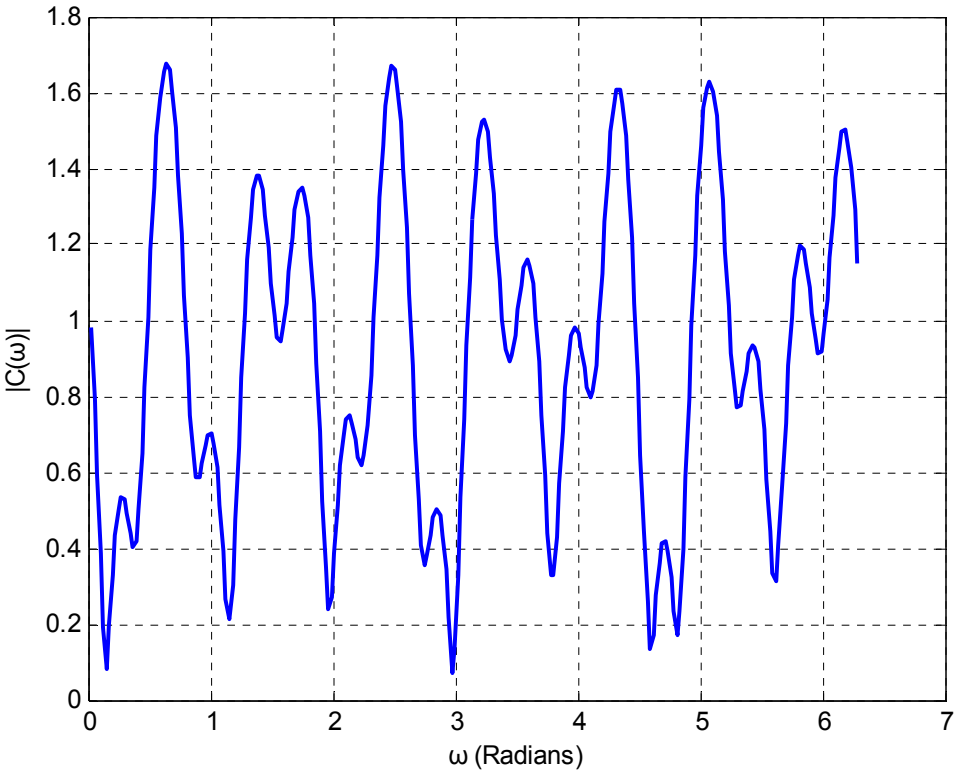

Figure 26. Snapshot of the modified SUI-3 channel frequency response used for the simulation.

After identifying the optimal threshold value, which was about 6 dB, we tested the standard OFDM receiver algorithm and the optimal estimation algorithm for various PAPR clipping conditions. Simulation results are shown in Figure 27.

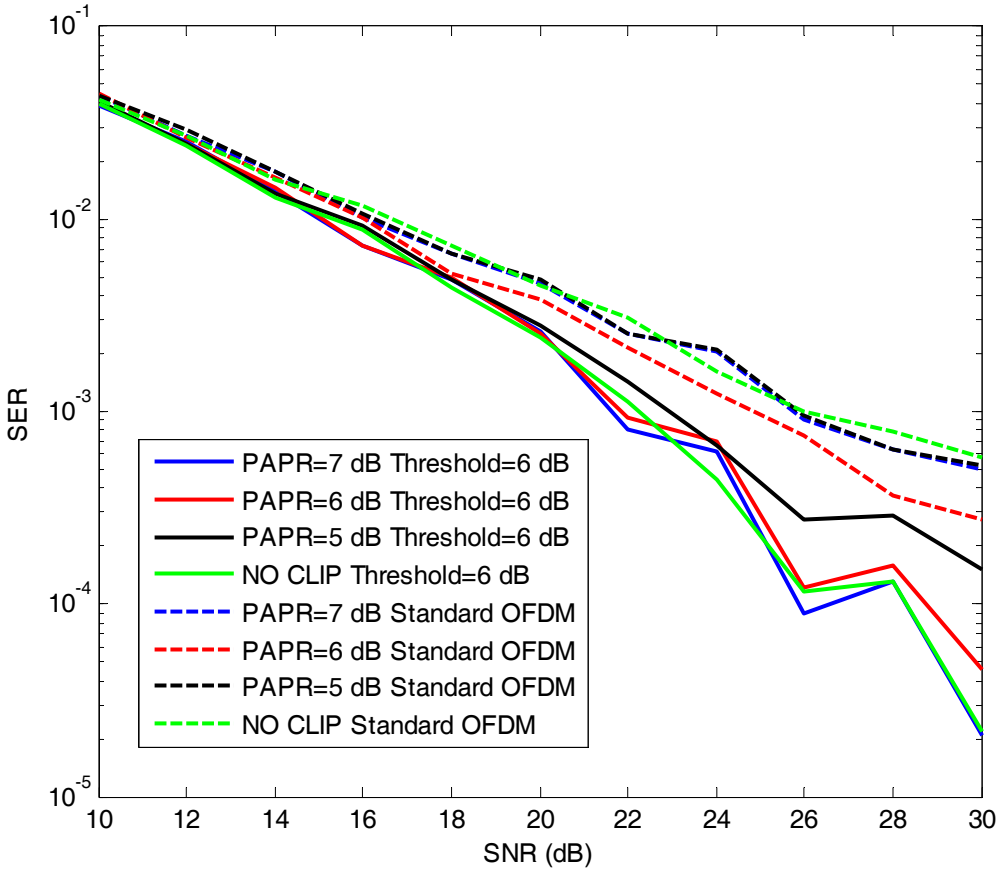

Figure 27. Comparison of the IEEE 802.16 standard QPSK SER with a standard OFDM receiver algorithm and optimal estimation (based on the Kalman filter) OFDM receiver algorithm for different cases of PAPR clipping for a modified SUI-3 channel.

In this final set of simulations, the standard algorithm (dashed line) and the proposed algorithm (solid line) performances are compared in terms of symbol error rate versus SNR value for different PAPR values expressed in dB. As previously, results show error rates increase with increased clipping levels. Results also show that the proposed optimal algorithm overall has better performances than those obtained with receivers which do not use the proposed algorithm.

THIS PAGE INTENTIONALLY LEFT BLANK

VI. CONCLUSIONS

The goal of this thesis was to study the null estimation method proposed in [1] and take it one step further. We proposed the optimal Kalman-based estimation method and implemented the scheme using the OFDM symbol architecture based on the 802.11a IEEE standard. Next, we extended the study to OFDM symbol architecture based on the 802.16 IEEE standard and real world application SUI-3 channel types.

A. SUMMARY

Research results derived in this thesis show that the CP can be replaced with zeros and that this technique gives the received signal a particular structure that can be used to recover the data associated with faded subcarriers. We assumed full knowledge of the noisy deep-fading channel and selected two types of OFDM signals, which were studied for various channel conditions in order to detect the optimal threshold and for different clipping values in order to reduce the PAPR effect. Results were compared to those obtained with standard pilot based techniques.

B. SIGNIFICANT RESULTS

The optimal estimation method considered in this work is based on the Kalman filter. The algorithm implemented appeared to be very robust and performed very well. Simulations using an OFDM signal based on IEEE standards 802.11a and 802.16 showed that the optimal estimation algorithm performed better than the standard OFDM receiver algorithm for various SNR conditions.

The optimal estimation method relies on the definition of a threshold in the frequency spectrum of the received signal, which separates subcarriers with high SNR from faded subcarriers with low SNR. Results showed that the SER varies when different threshold values are selected. Hence, the best SER can be obtained with the appropriate threshold, which is dependent on the SNR.

The algorithm was easily modified to accommodate and deal with the problem of PAPR that OFDM introduces. During the simulations, we used different values of clipping, and the results showed that the optimal estimation performed very well.

C. NECESSITY FOR DATA RECOVERY IN MARITIME OPERATIONAL APPLICATIONS

This modification of the OFDM structure makes it robust in difficult environments where there is no LOS and the channel has considerable fading. Such a scenario may occur with small boats or deployed troops on the ground communicating with each other in the presence of hills and NOLOS. In addition, this modification could be of interest in underwater acoustic data communications where one deals with sea bottom and surface reverberations and reflection effects [9].

D. RECOMMENDATIONS FOR FUTURE WORK

There are numerous areas available for future work with this thesis. First of all, instead of using ZP for CP, the algorithm can be used with a random prefix sequence that enables synchronization between transmitter and receiver.

Secondly, the MATLAB algorithm implemented in this work is generic and can accommodate different types of OFDM signals, thereby extending the range of applications.

Thirdly, the algorithm can be modified for different channel models, such as Hata, Walfish-Ikegami or Erceg models, which are commonly used.

Fourth, a potential channel estimation algorithm can be implemented, based on the optimal estimation method using the Kalman filter, and performance can be tested for various conditions.

LIST OF REFERENCES

[1] A. G. Stranges, "Blind equalization and fading channel signal recovery of OFDM modulation," Master's thesis, Naval Postgraduate School, Monterey, California, 2011.

[2] J. Wang, J. Song and L. Yang, "A novel equalization scheme for ZP-OFDM system over deep fading channels," *IEEE Trans. on Communications*, vol. 56, no. 2, pp. 249–252, 2010.

[3] R. Cristi, unpublished notes, November 2011.

[4] R. Marks, "IEEE Standard 802.16: A technical overview of the WirelessMAN™ air interface wireless access," IEEE C802.16-02/05, June 2002.

[5] G. C. Goodwin, K. S. Sin, "Stochastic systems," in *Adaptive Filtering Prediction and Control*, Upper Saddle River, NJ: Prentice-Hall, 1984, pp. 248–262.

[6] V. Erceg, K.V. S. Hari, M.S. Smith, D.S. Baum, K.P. Sheikh, C. Tappenden, J.M. Costa, C. Bushue, A. Sarajedini, R. Schwartz, D. Brandlund, T. Kaitz and D. Trinkwon, "Channel models for fixed wireless applications," IEEE 802.16.3c-01/29r4, July 2001.

[7] R. V. Nee and R. Prasad, "The peak power problem," in *OFDM for Wireless Multimedia Communications*, Boston: Artech House, 2000, pp. 119–131.

[8] R. Jain, "Channel models: A tutorial," V1.0, February 2007. Available: http://www.cse.wustl.edu/~jain/cse574-08/ftp/channel_model_tutorial.pdf.

[9] K. Tuy, D. Fertonani, T. Duman, M. Stojanovic, J. Proakis and P. Hursky, "Mitigation of intercarrier interference for OFDM over time-varying underwater acoustic channels," *IEEE J. of Oceanic Engineering*, vol. 36, no. 2, pp. 156–171, 2011.

THIS PAGE INTENTIONALLY LEFT BLANK

INITIAL DISTRIBUTION LIST

1. Defense Technical Information Center
   Ft. Belvoir, Virginia

2. Dudley Knox Library
   Naval Postgraduate School
   Monterey, California

3. Chairman, Code EC
   Department of Electrical and Computer Engineering
   Naval Postgraduate School
   Monterey, California

4. Professor Roberto Cristi
   Department of Electrical and Computer Engineering
   Naval Postgraduate School
   Monterey, California

5. Professor Monique P. Fargues
   Department of Electrical and Computer Engineering
   Naval Postgraduate School
   Monterey, California

6. Professor Tri Ha
   Department of Electrical and Computer Engineering
   Naval Postgraduate School
   Monterey, California

7. Embassy of Greece
   Office of Naval Attaché
   Washington, District of Columbia

8. LT Konstantinos Charisis
   Hellenic Navy General Staff
   Athens, Greece